energies

MDPI

Review

Polyimide Copolymers and Nanocomposites: A Review of the Synergistic Effects of the Constituents on the Fire-Retardancy Behavior

Shengdong Xiao, Caroline Akinyi, Jimmy Longun and Jude O. Iroh *

Materials Science and Engineering Program, Department of Mechanical and Materials Engineering, College of Engineering and Applied Science, University of Cincinnati, Cincinnati, OH 45221, USA; xiaosg@mail.uc.edu (S.X.); akinyicj@mail.uc.edu (C.A.); jlongun2008@gmail.com (J.L.)
* Correspondence: irohj@ucmail.uc.edu

Abstract: Carbon-based polymer can catch fire when used as cathode material in batteries and supercapacitors, due to short circuiting. Polyimide is known to exhibit flame retardancy by forming char layer in condensed phase. The high char yield of polyimide is attributed to its aromatic nature and the existence of a donor–acceptor complex in its backbone. Fabrication of hybrid polyimide material can provide better protection against fire based on multiple fire-retardancy mechanisms. Nanocomposites generally show a significant enhancement in mechanical, electrical, and thermal properties. Nanoparticles, such as graphene and carbon nanotubes, can enhance flame retardancy in condensed phase by forming a dense char layer. Silicone-based materials can also provide fire retardancy in condensed phase by a similar mechanism as polyimide. However, some inorganic fire retardants, such as phosphazene, can enhance flame retardancy in gaseous phase by releasing flame inhibiting radicals. The flame inhibiting radicals generated by phosphazene are released into the gaseous phase during combustion. A hybrid system constituted of polyimide, silicone-based additives, and phosphazene would provide significant improvement in flame retardancy in both the condensed phase and gas phase. In this review, several flame-retardant polyimide-based systems are described. This review which focuses on the various combinations of polyimide and other candidate fire-retardant materials would shed light on the nature of an effective multifunctional flame-retardant hybrid materials.

Keywords: flame-retardant polymers; polyimide; nanocomposites; synergistic fire retardants; phosphazenes

Citation: Xiao, S.; Akinyi, C.; Longun, J.; Iroh, J.O. Polyimide Copolymers and Nanocomposites: A Review of the Synergistic Effects of the Constituents on the Fire-Retardancy Behavior. *Energies* **2022**, *15*, 4014. https://doi.org/10.3390/en15114014

Academic Editor: Andres Siirde

Received: 19 April 2022
Accepted: 24 May 2022
Published: 30 May 2022

1. Flame Retardancy

Polymeric materials play a critical role in the industry because of their attractive characteristics, such as low density, chemical resistance, and outstanding mechanical properties. Carbon-based polymers backbones are mostly combustible. For a general-purpose application, this is not a fatal flaw. However, the flammability of polymeric materials might severely limit their application in the aerospace, transportation, and electronics industries. Also, in the daily life, one main source of fire hazard is from short circuiting of electric devices. Many polymeric materials are considered to be combustibles under such a hazardous condition. On the other hand, some polymers, including polyimide, have shown great promise for use in energy storage applications. Therefore, it is necessary to understand the flame-retardant behavior of polyimides in order to fully utilize them in a safe and effective manner.

In order to fully describe the flame retardancy of polymeric materials, the mechanism of polymer combustion must be well understood [1]. The traditional model of combustion is known as combustion triangle which suggests that the basic combustion reaction involves three keystones. Polymer materials play the role as combustibles while oxygen in the air is

the combustive fuel. The heat generated during combustion will raise temperature of the polymer leading to bond scissions which produces volatile polymer in the form of gas. If the heat released during combustion can reach a critical level, a combustion cycle would be established and maintained. An effective flame-retardant material would inhibit or break this cyclic process.

A recent study described the polymer combustion behavior as a kinetic fire loop model [2]. The fire loop model, initially reported by Emmons [3], is regarded as a more precise description for the combustion behavior of polymer. Combustion of polymer involves two sequences: pyrolysis and oxidation (shown in Figure 1). Pyrolysis, occurring in condensed phase, is the crucial step in the loop and generates the fuel for combustion. While in gaseous phase, the oxidation of fuel flux affects the pyrolysis via heat feeding. Hence, the aim of a flame-retardant system should be the reduction of the rate of one or both reactions. In a self-sustained combustion process, a balance between the generation and consumption of volatile fuel should be established as shown in Equation (1). In the presence of flame retardant, the steady-state pyrolysis product concentration, $[G]_{SS}$ should be lowered to the flammable limit to cease the fire.

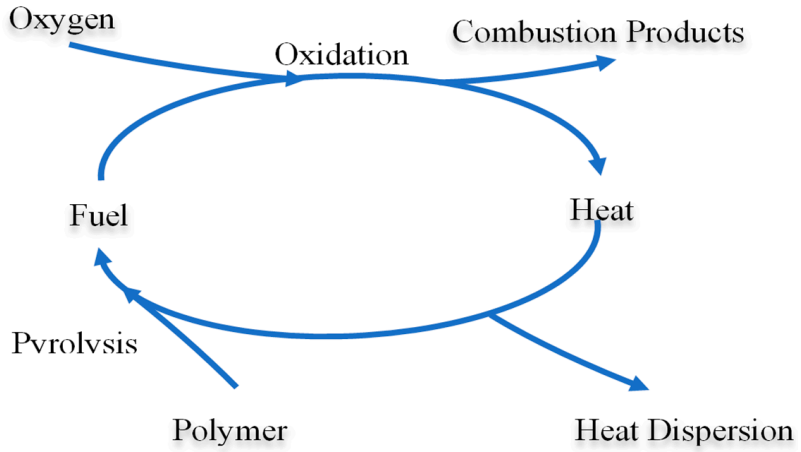

Figure 1. Representation of the fire loop model [2].

Flame retardants in condensed phase will lower the production rate of flammable polymer volatiles by introducing an extra reaction of the polymer into loops. On the other hand, flame retardant that acts in gaseous phase will react with pyrolysis products and affect the whole process of combustion by consuming more volatile fuel. The controlled fire loop model is described by Equation (2). One key finding from this study is the suggestion that restraining both reactions can result in reduction of the overall combustion process since the synergetic reduction is multiplicative and not additive. Therefore, effective flame-retardant systems should ensure the reduction of the rate of reaction in both the condensed and gaseous phases.

$$\frac{d[G]_{SS}}{dt} = k_{OX}[G]_{SS} - k_G[P]_{SS} = 0 \quad (1)$$

where the v_{OX} and k_{OX} is the rate and rate constant of fuel (pyrolysis product) oxidation, $[OX]$ is the concentration of the combustion products, $[P]_{SS}$ and $[G]_{SS}$ are the steady state polymer concentration and pyrolysis product concentration in volume [2].

$$\frac{d[G]_{SS}}{dt} = k_{OX}[G]_{SS} + k_{FRG}[FRG][G]_{SS} - k_G[P]_{SS}\frac{k_G}{k_G + k_{FRC}[FRC]} = 0 \quad (2a)$$

$$[G]_{SS} = k_G[P]_{SS}\frac{k_G}{k_G + k_{FRC}[FRC]}\frac{1}{k_{OX} + k_{FRG}[FRG]} \quad (2b)$$

where $[FRC]$ and $[FRG]$ are the concentration of flame retardants in condensed phase and gaseous phase, respectively [2].

Different approaches can be applied to gain flame retardancy based on the model mentioned above. The first one is called physical action. In this case, no chemical reaction is directly involved in the retardancy process. For instance, by cooling, diluting the concentration of fuel gas, or forming of a protective layer, combustion could be inhibited. On the other hand, some fire-retardant agents can react during polymer combustion and interfere with the oxidation process. This type of mechanism is referred as the chemical action.

One frequently reported physical flame-retardant model is called heat sink. A flame-retardant agent, such as hydrated alumina or magnesium hydroxide, could release water vapor under high-temperature exposure [4,5]. Therefore, heat would be consumed and then temperature could drop to a level lower than the polymer combustion temperature. Additionally, the released inert water vapor would dilute the concentration of combustible gas.

Chemical flame retardancy is usually associated to chain scission. Traditional halogen fire-retardant agents would release halogen radicals to couple with highly reactive radicals forming inert molecules. Due to the reduction of fuel, the combustion cycle cannot be sustained. The flame retardants can strongly accelerate the polymer backbones scissions causing polymer to drip away from combustion area. Some fire retardants can catalyze the formation of carbonized or vitreous layer on the surface of the matrix material. This layer will act as a protection barrier.

Flame retardants can also be classified into two categories based on their methods of addition: reactive and additive flame retardants. Reactive flame retardants are introduced into materials in the synthesis stage. They are used as monomer, precursor polymers, or grafting agents. On the contrary, additive fire retardants do not react with polymer directly. They are generally physically mixed with materials. Only under high-temperature condition, do the additive fire retardants become active.

The synergistic effect between flame retardants can be achieved via proper combinations of different mechanism [6,7]. It is a smart approach to ensure the efficiency of flame retardants without sacrificing other properties. Zanetti et al. reported a hybrid polypropylene filled with montmorillonite (MMT) nanoparticles and decabromodiphenyl oxide (DB)-antimony trioxide (AO) [6]. The average heat-release rate of different compositions was measured by cone calorimeter and shown in Figure 2. A decent reduction was achieved from addition of single type of flame retardant. Both decabromodiphenyl oxide and antimony trioxide are flame-retardant additives which are active in gaseous phase. However, a combination of those two even weaken the efficiency of flame retardancy. On the other hand, system containing clay with either AO or DB showed significant reduction in heat-release rate. The highest reduction of the heat-release rate was observed in the system containing all flame-retardant additives.

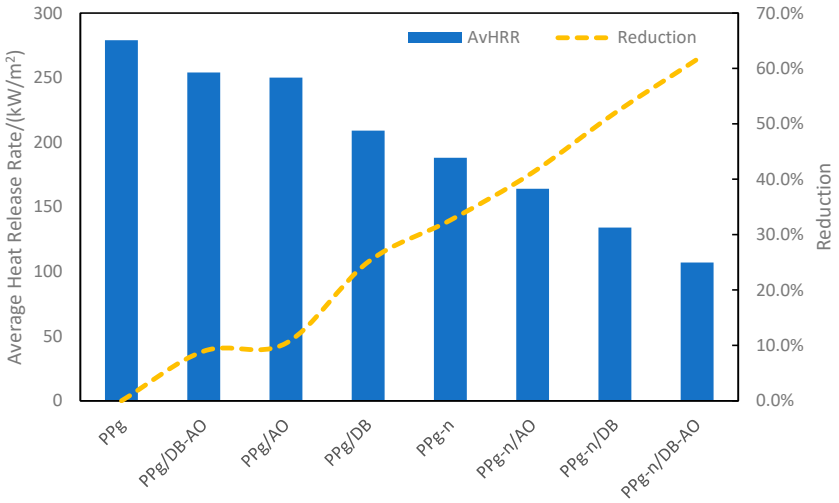

Figure 2. Average heat-release rate of flame-retardant polypropylene and reduction on HRR (PPg: polypropylene-graft-maleic anhydride, PPg-n: polypropylene with montmorillonite clay) [6].

2. Polyimide

Polyimide is a well-known high-performance polymer material with a wide range of properties that are desired in many commercial applications [8]. For instance, polyimides can effectively resist chemical degradation. Hence, they can be used as coating materials [9–11]. Polyimides have relatively low concentration of free charge carries, making them suitable for micro electrical engineering application as an excellent candidate of insulating materials [12–18]. To meet the specific requirement for use in electronic packaging, proper changes to the preparation procedure must be made. One of the commonly preferred approaches to lowering the dielectric properties of polyimide is by fluorination [19–26]. Fluorinated polyimides have effectively higher hydrophobicity, free volume, and polarizability.

Another frequently used modification strategy is the introduction of nanofillers [27,28], such as graphene. Marashdeh, et al. reported graphene reinforced polyimide composites [12,28]. In these studies, varying weight fractions of graphene were incorporated into the polyimide matrix. It was shown that increasing the weight fraction of graphene resulted in a significant increase in the dielectric constant and that the addition of 30 wt.% graphene resulted in about 55,000 times increase in the dielectric constant over that for neat polyimide.

Polyimide is also believed to be a promising cathode material for energy-storage devices [29–31]. Since the 1960s, scientists have developed organic electrode materials, such as dichloroisocyanuric acid [32]. Researchers believe that the presence of a conjugated double bond, similar to that in an aromatic phenyl ring, could promote an electrochemical redox process. Moreover, compared to ceramic materials, polymer materials are preferred because of their excellent strength and relatively low density [33–36]. With the addition of inorganic fillers, it is feasible to produce high-power density devices. Weidong Sun et al. have evaluated the energy storage properties of polyimide/barium titanium oxide, PI/$BaTiO_3$ composites. The dielectric permittivity of the composite was significantly changed in the presence of nanoparticles [35].

Fire hazard caused by potential short circuit or overuse is considered to be a major concern in the electronic industry. On the other hand, polyimide can be classified as a high temperature polymer [37–43]. Generally, polymers with a continuous service temperature greater than 150 °C are known as high-temperature polymers. Based on the presence of heterocyclic imide ring in the backbone, polyimides have characteristically high thermal stability [43–46]. Moreover, the char yield of polyimide under high-temperature exposure in inert atmosphere is very high $\geq$55%. Based on these unique characteristics, polyimides have become outstanding candidates for developing flame-retardant materials.

Büger et al. determined the degradation mechanism of polyimide, as shown in Scheme 1 [47]. Heat pyrolysis of polyimide in air atmosphere starts around 550 °C with rupture of imide ring structure. Once the temperature reaches around 700 °C, the decomposition products would become mostly planar polyaromatics, which provide transient protection in the form of char layer. Finally, continuous ramping of temperature will eventually lead to the failure of the polyimide residues.

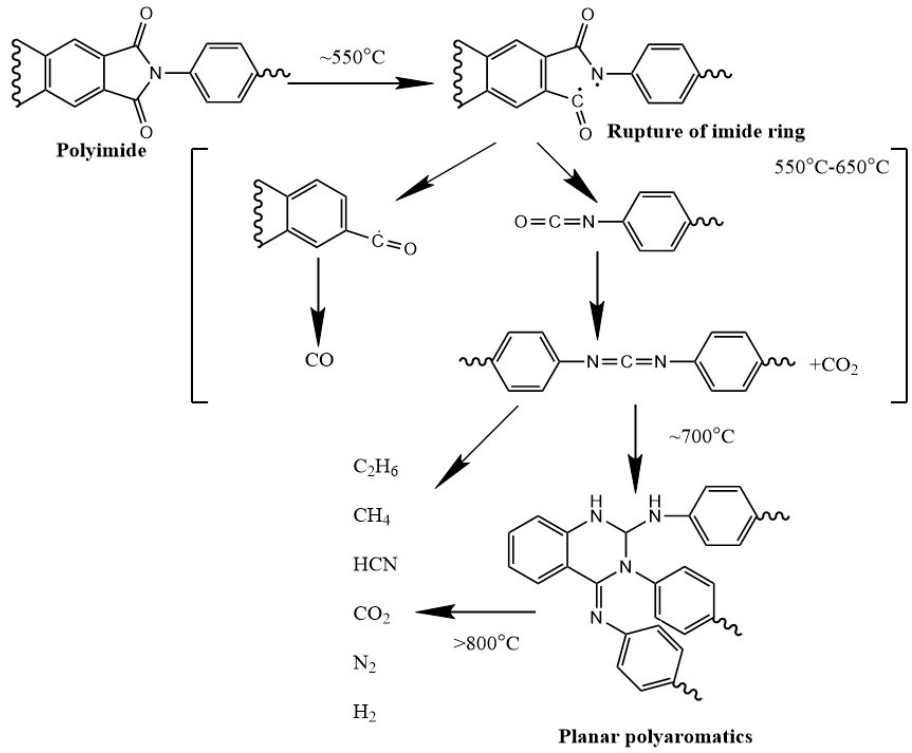

Scheme 1. Representation of the degradation mechanism of polyimide in air atmosphere [47].

Polyimide is usually synthesized by a two-step process [48–57]. The first step is the synthesis of the precursor, poly(amic acid). In the second step, chemical or thermal method is used to cure poly(amic acid), by a process called imidization, to produced fully imidized polyimide [54]. Imidization involves cyclization and dehydration of poly(amic acid). With the aid of Fourier transfer infrared spectroscopy (FT-IR), the extent of imidization can be determined. For a giving imidization temperature and time, the extent of imidization can be determined by normalizing the area of the imide carbonyl absorption peak with the area of the phenyl ring absorption peak whose intensity remains constant during imidization and dividing this ratio by the peak intensity ratio for the fully cured polyimide [55,56]. It is believed that partially cured polyimide will undergo further imidization when heated to a temperature $\geq$300 °C, thereby releasing water vapor into gaseous phase. During combustion, the released water vapor will dilute the flammable species [57]. Based on their thermal properties, partially imidized polyimides can serve as excellent alternative to smart flame-retardant materials.

3. Carbon-Based Nanofiller

Carbon-based nanoparticles have been of heightened interest to scientists and engineers recently. Nanofillers such as graphene and carbon nanotubes (CNT), are used to modify the mechanical, electrical, and thermal properties of different materials. It is believed that only a low loading per cent is required to achieve significant flame retardancy for these types of nanofillers. Flame retardancy of nano materials is generally effective in the condensed phase [58–71]. CNT [72–76] and graphene can form of a dense char layer covering of various polymer materials.

Kashiwagi et al. reported the reinforcement of poly(methyl methacrylate) (PMMA) by single-walled carbon nanotube (SWNTs) [77]. The flame retardancy of the composite was analyzed by using the cone calorimeter. The heat-release rate and mass-loss rate of the samples were severely suppressed in the presence of SWNT. Neat PMMA showed a maximum heat-release rate higher than 1200 kW/m^2. However, with addition of 0.5% SWNT, the heat-release rate was lower than 600 kW/m^2. Also, the mass-loss rate of neat

PMMA was higher than 35 g/(m^{2}s). With addition of SWNT (0.5%), the mass-loss rate of PMMA was decreased to around 10 g/(m^{2}s). In the neat polymer samples, the whole structures were observed to be burnt out without any residues. However, at low SWNT loading per cent, partially protective char was formed. A dense protective layer was formed when SWNT loading was equal to or greater 0.5%. In these cases, no cracking was observed.

Another commonly used nanofiller is graphene. As a monolayer carbon 2D material, graphene or graphene oxide could provide remarkable property enhancement in the composites [78–83], such as improved thermal stability and fire retardancy. Graphene usually decomposes around 600 °C in air but can remain stable up to 800 °C in inert atmosphere [84–93].

Unlike neat amorphous polyimide, the presence of graphene can be detected by X-ray diffraction analysis. Longun et al. reported a series of study on nano graphene sheets/polyimide nanocomposites [94–97]. Wide angle X-ray diffraction (WAXD) was used to evaluate the dispersion and presence of graphene in the polyimide matrix. There are two important diffraction peaks to be noticed. The peak located at 26.5° (d = 3.36 Å) indicates the presence of graphene platelets and it was observed in both neat graphene samples and PI-GR composites. Figure 3 shows the graphene peak intensity increases with the graphene fraction in composites. Another peak at 5.65° (d = 15.63 Å) was observed in composites samples only and it is due to the interaction of graphene with polyimide matrix [94–97]. The broad peak locating around 18.87° (d = 4.70 Å) was found in spectrum of polyimide and indicates the amorphous hallow.

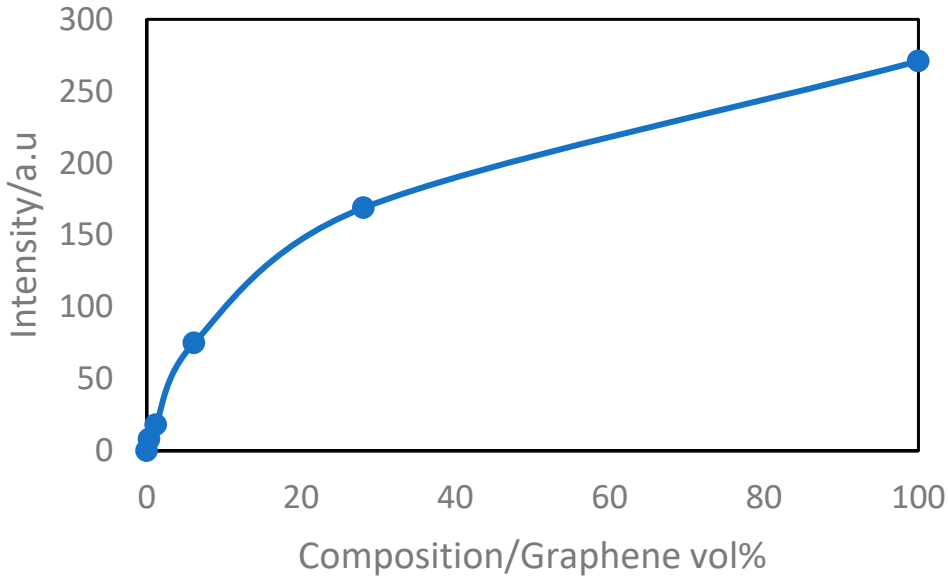

Figure 3. WAXD analysis showing the dependence of graphitic carbon peak intensity (at 2θ angle of 26.5° (d = 3.36 Å) for graphene/PI composites, on the weight fraction of graphene [94–97].

Also, functionalized graphene (FG) or graphene oxide (FGO) would have a better dispersion in the polymer matrix. This is crucial to ensure performance enhancement. For instance, Bao et al. reported a graphene oxide functionalized with cyclophosphazene incorporated with polystyrene [86]. Better dispersion of FGO was observed compared to the neat graphene. The fire-retardancy results are shown in Figure 4. It shows the enhancement in thermal stability in the presence of FGO. In fire-safety tests, it was reported that the addition of 3 wt.% FGO resulted in a 53% decrease in the peak heat-release rate when compared to neat polystyrene, PS. The total heat release for this system was also decreased by 33% over that for the neat PS.

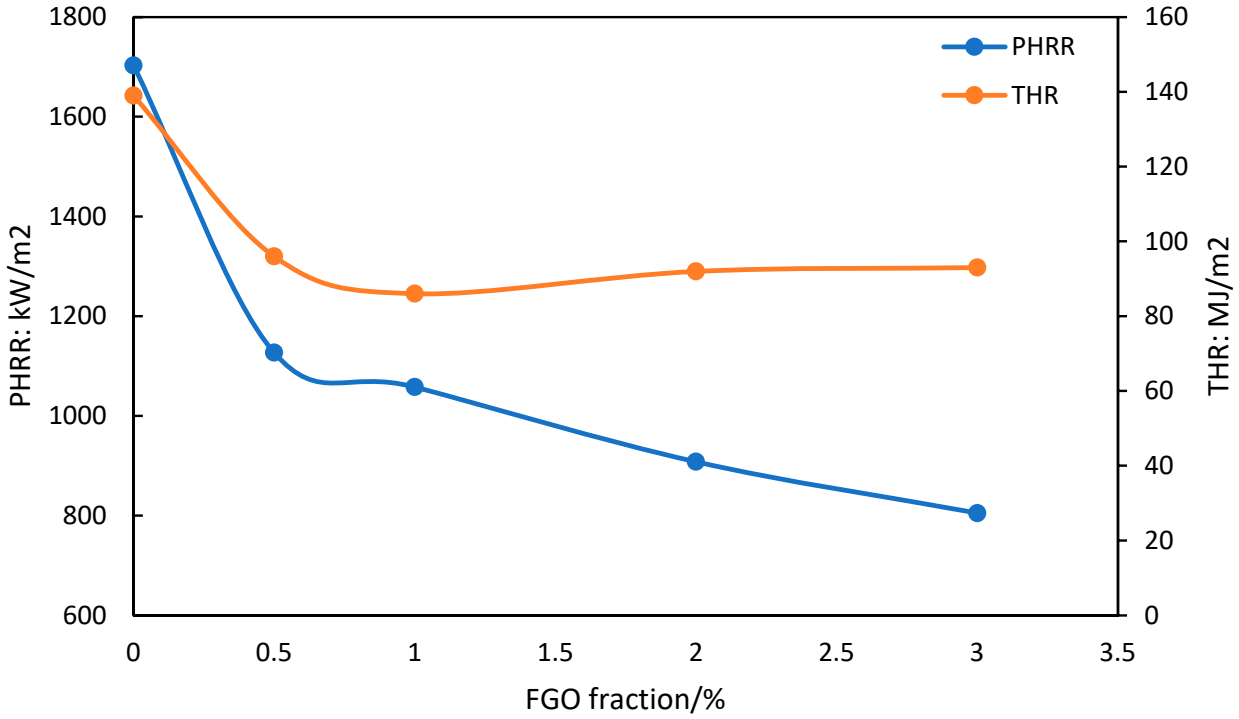

Figure 4. Fire-safety results obtained from cone calorimetry (heat flux of 35 kW/m^2 in nitrogen), showing the effect of FGO weight fraction on the peak heat-release rate (PHHR) and total heat release (THR) for FGO/PS nanocomposites [86].

Zuo et al. reported polyimide/graphene oxide/montmorillonite (P/G/M) aerogel composites [98]. Montmorillonite (MMT) clay nanoparticle is capable of enhancing the flame retardancy of polymer matrix. The presence of graphene oxide will overcome the possible flaw of heavy aggregation of MMT through a synergistic dispersion effect. The measured LOI values confirm the synergistic effect between MMT and graphene oxide. The combination of PI/GO (5 wt.%)/MMT (10 wt.%) has LOI of up to 55 compared to neat PI of 44.6 and PI/GO of 46 and PI/MMT of 45.5.

In a recent report, Akinyi et al. studied the flammability of polyimide and graphene/polyimide nanocomposites [87,99]. Multilayered graphene sheets with thickness ranging from 50–100 nm was used in these studies. Multilayer graphene is cheaper and more processable than single-layer graphene. The nanocomposites contained up to 50 wt.% graphene. The presence of graphene in the nanocomposite was confirmed by FT-Raman spectroscopy. The absorption peaks for graphene were observed at 1360 cm^{-1} and 1540 cm^{-1}. Absorption peaks at 1790 cm^{-1} and 1390 cm^{-1} were attributed to the imide ring. In Figure 5, it was shown that imide ring intensity increases with the fraction of graphene in composites Elemental composition analysis based on EDAX was reported in Figure 6 [99]. After combustion, the nitrogen and oxygen fractions decreased while a significant increase in the carbon fraction was observed [99]. As shown in the derivative weight-loss DTA curves, there are multiple stages of decomposition of PI and PI-GR composites [99]. The derivative weight-loss curve of neat PI and graphene as well as graphene/polyimide composites are shown in Figure 7a,b. Figure 7a shows that the first stage of decomposition of polyimide starts from 600 °C and extends to 650 °C. This initial degradation profile is associated with the decomposition of the imide ring. At about 700 °C, the polyimide char starts to fail. At a higher temperature of about 800 °C, another decomposition stage is observed both in neat graphene and in polyimide-graphene composites and is attributed to the degradation of graphitic carbon in graphene. Figure 7b shows the effect of graphene on the decomposition of the imide ring. It is clearly shown that the higher the

graphene concentration, the better the protection provided to the imide ring (Figure 7b (inset)). This phenomenal behavior is attributed to the ability of graphene to act as a heat sink and shield over the imide ring. It is very noteworthy, therefore, that the presence of graphene strongly influenced the failure of polyimide ring and polyimide char. The calculated char degradation rate is plotted as a function of graphene weight fraction and is shown in Figure 8. The trend of degradation rate shows that the presence of both graphene and polyimide in the composite resulted in overall reduction of the char degradation rate for both the neat PI as well as for graphene. Indeed, the lowest char degradation rate occurred in the composite containing 30 wt.% of graphene (Figure 8). Akinyi et al. and others also determined the heat-release rate based on TGA and DSC analysis and by using Equations (3) and (4) [99,100].

$$\Delta H = \int_{T_1}^{T_2} \left(\frac{\partial H}{\partial T}\right)_p dT = \int_{T_1}^{T_2} C_p dT. \quad (3)$$

$$\dot{q} = \Delta H \times \dot{m}_{fuel} \quad (4)$$

where ΔH is the total enthalpy change of degradation and $\dot{m}_{fuel}$. is the weight-loss rate from TGA and DTA. They showed that the total heat of degradation decreased remarkably by an order of magnitude from 1.1 kJ/g for the neat PI to 0.1 kJ/g for PI reinforced with 50 wt.% of graphene [99].

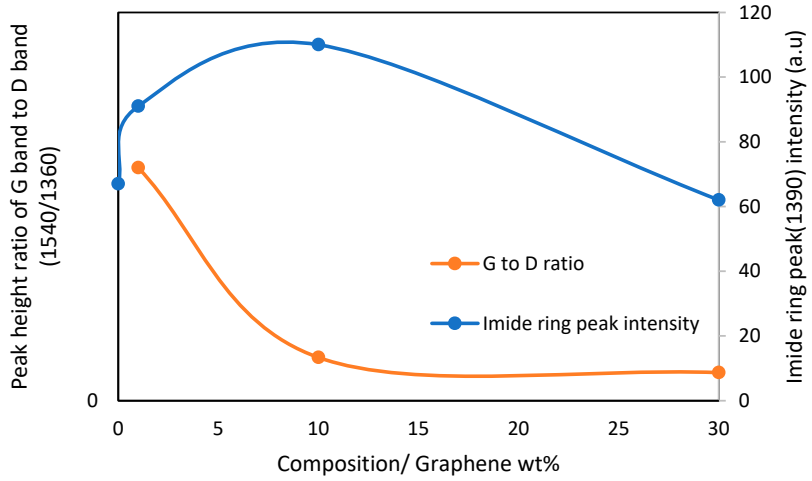

Figure 5. Dependence of the FT Raman imide ring peak intensity (1390 cm^{-1}) and ratio of peak intensity of G band to D band on graphene wt.% [87].

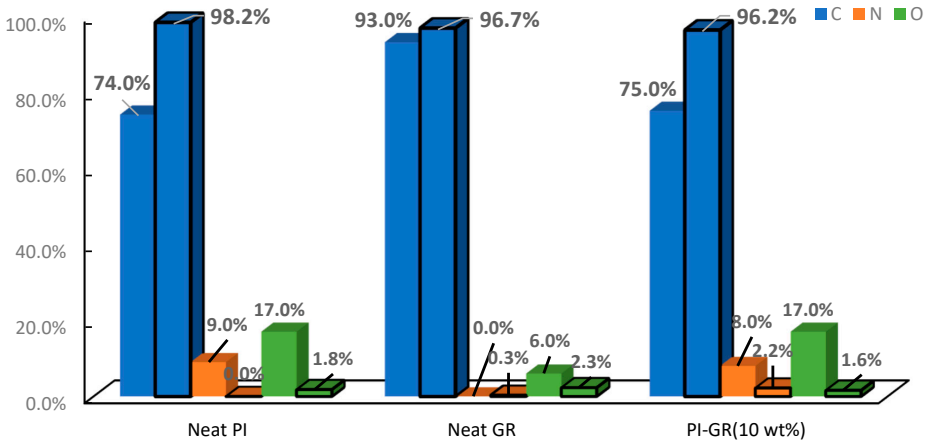

Figure 6. Elemental composition (blue bar: carbon, orange bar: nitrogen, and green bar: oxygen) of PI, graphene and PI/GR (10 wt.%) based on EDAX data (black outline: after combustion) [87,99].

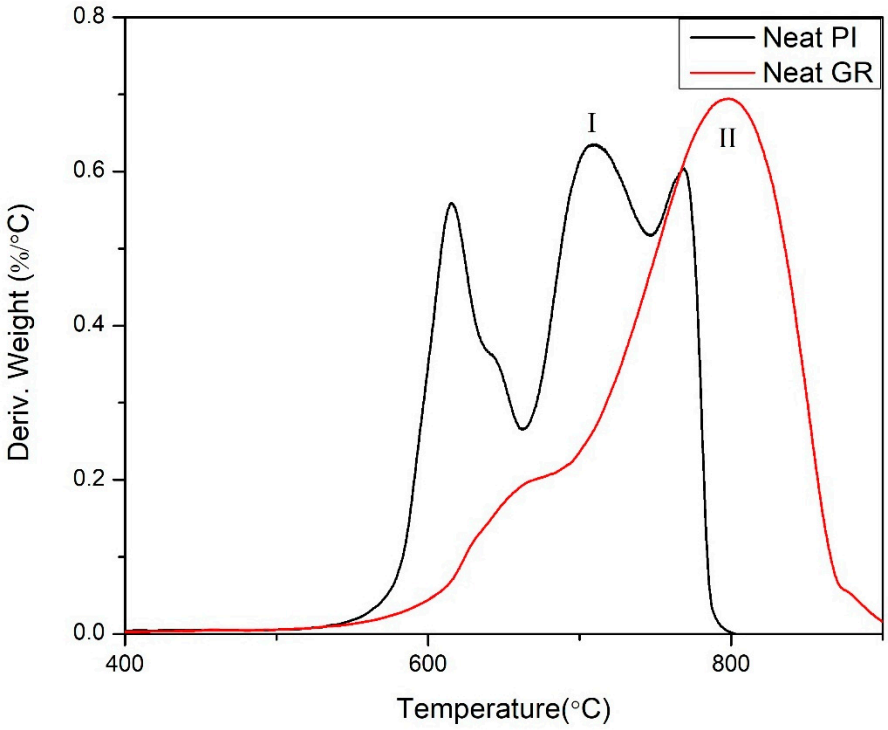

(**a**)

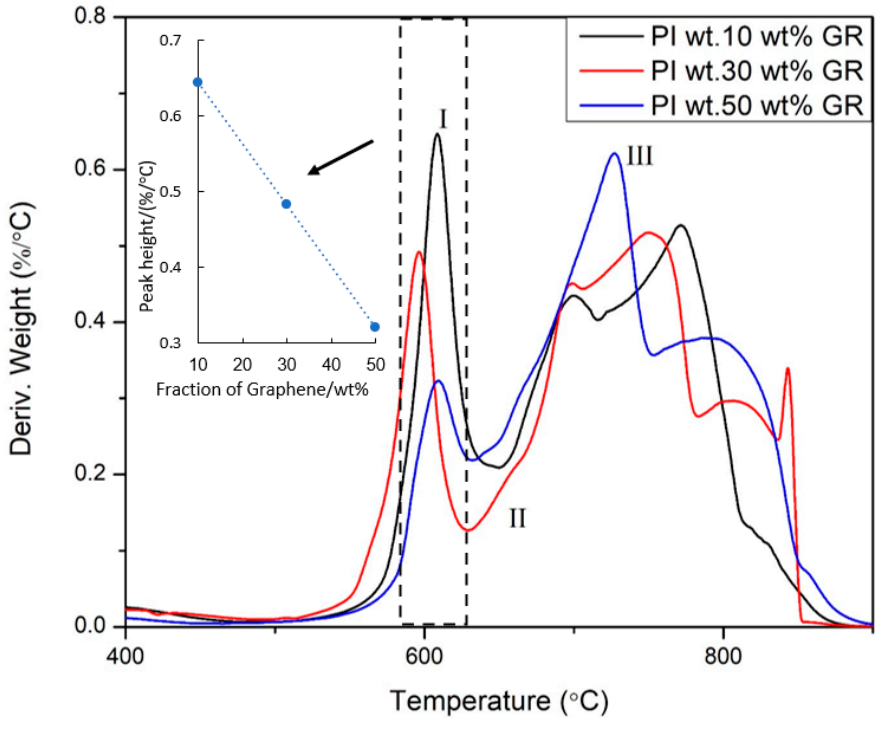

(**b**)

Figure 7. (**a**) DTA curves of (I) Neat PI and (II) neat graphene tested in air with a heat rate of 30 °C/min [99], (**b**) DTA curves of PI-GR composites: (I) PI-10% graphene, (II) PI-30 wt.% graphene, and (III) PI-50 wt.% graphene and comparison of imide decomposition (~600 °C) peak height (tested in air with a heat rate of 30°C/min) [99].

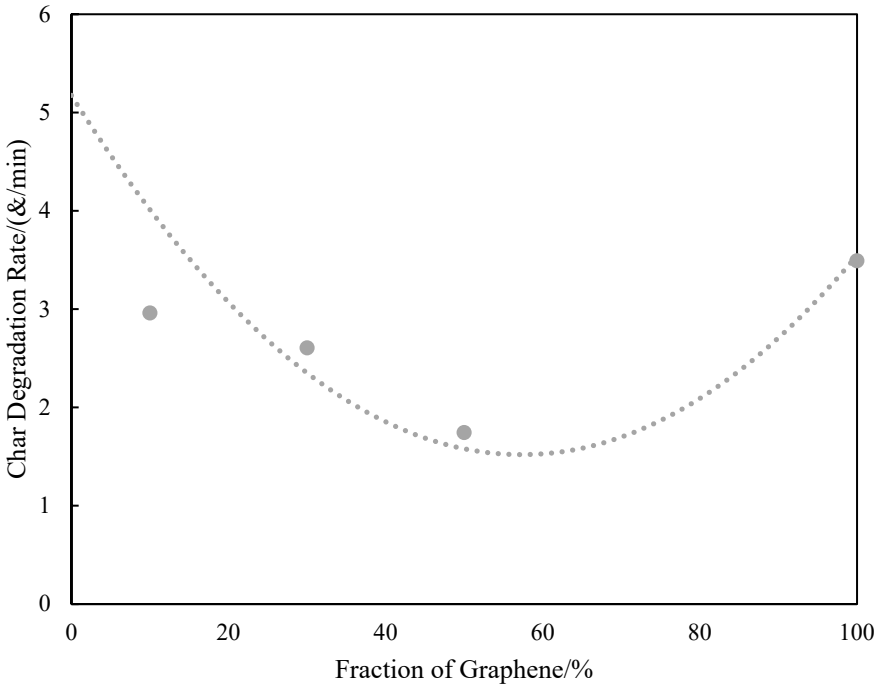

Figure 8. Dependence of the char degradation rate for PI/graphene nanocomposites on wt.% graphene [101].

4. Phosphazene

Halogen fire retardants used to be the most widely used reactive flame-retardant additives. Frequently used halogenated additives are shown in Scheme 2. Those additives usually contain up to 10 halogen atoms which can be released into the gaseous phase as free radical (X•). Halogen radical will couple with hydrogen radicals to form non-flammable species HX which would dilute the fuel gases in the form of protective gaseous coating. However, the traditional halogen flame retardants have a serious flaw. Although, this type of flame retardant is effective and only small amount of addition is required to give high flame retardancy. Halogenated fire-retardant agents release toxic gaseous materials during combustion. Therefore, they are prohibited in most countries [102–105].

Phosphorus based additives have similar flame-retardancy mechanism as halogenated fire retardants. These additives can evaporate into the gas phase as active phosphoxy radicals (PO_2•, PO•, and HPO•) which the act as scavengers of hydrogen H• and hydroxy OH• radicals to effectively inhibit combustion. They are, indeed, effective combustion inhibitors. It was reported that phosphorus containing radicals have 5 times higher flame retardancy than bromine and 10 times higher than chlorine radicals [106–112]. Red phosphorus is a common option of flame-retardant materials for polyesters, polyamides, and polyurethane [113–115]. It is considered to be very effective as a high-concentration source of phosphorus. Another frequently used inorganic compound is ammonium polyphosphate (APP). The best performance of APP is achieved when incorporated with oxygen/nitrogen-containing polymer. The product of pyrolysis of APP could catalyze the self-charring of polymer [116–118].

Phosphazenes are one class of organic compounds which has a double bonds linkage between phosphorus (V) and nitrogen, with the formula RN = $P(NR_2)_3$. With the aid of in-situ FT-IR spectroscopy, several authors have demonstrated both the condensed- and gas-phase fire-retardant mechanisms for cyclophosphazene and its derivatives [119–121]. The thermal oxidation of cyclophosphazene involves two important steps. Cleavage of the P-O-C bonds occurs in the temperature range of 250 °C–300 °C depending on the pendant group on the phosphazene ring. CO_2 and H_2O are released during this

process. Meanwhile, P-O-P bond will be formed by condensation. The condensation of phosphazene will also release water as shown in Scheme 3. This condensed structure will remain intact until the temperature reaches 500 °C. The P=N bond starts to fail around 300 °C–350 °C, thereby releasing NH_3, N_2, and inhibitor radicals. Once the P-O-P linkage fails, the fire-extinguishing radicals, such as PO_2•, PO•, and HPO•, will then be released into gaseous phase.

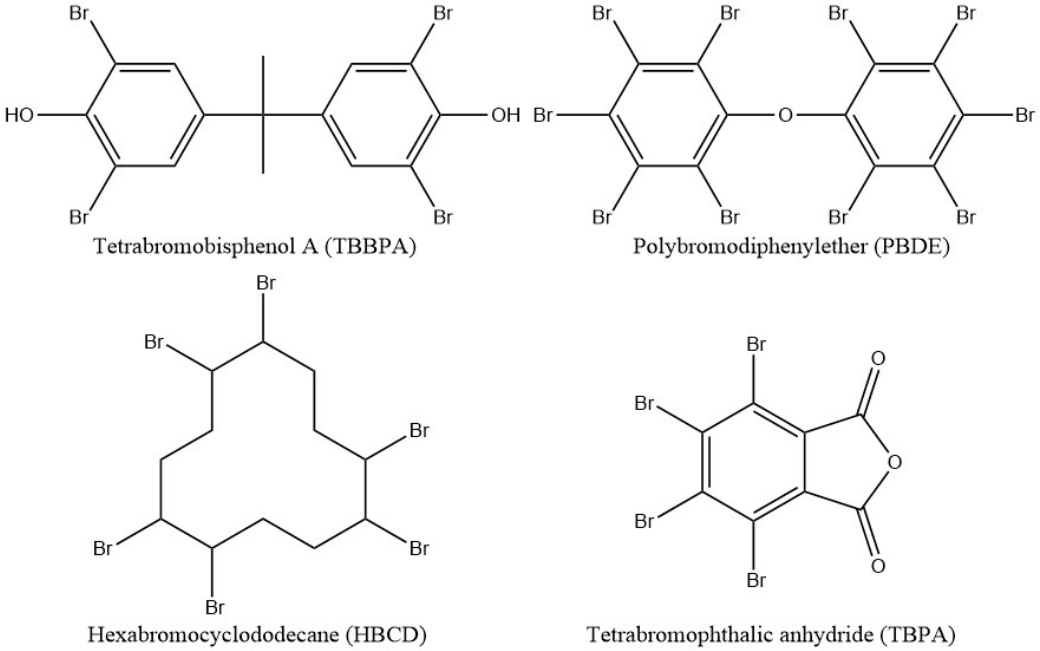

Scheme 2. Examples of the traditional halogenated flame retardants.

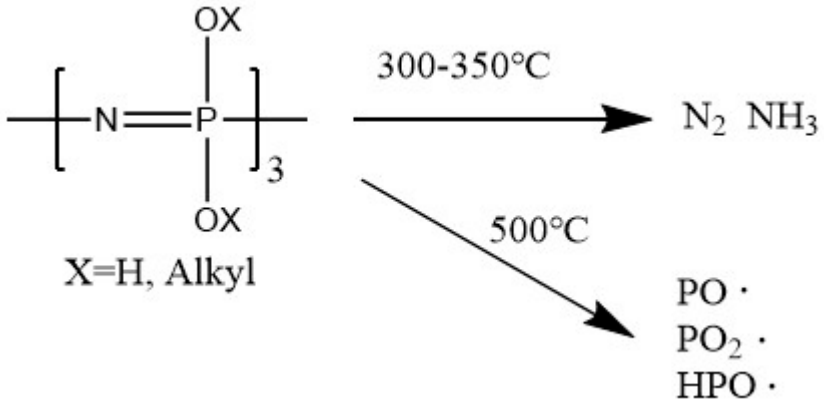

Scheme 3. Representation of the decomposition products for cyclophosphazene [119].

Phosphazenes are frequently inserted into polymer matrix to enhance the thermal properties or flame retardancy. It has characteristic outstanding thermal stability [122–132]. Also, the P-N group is more environmentally-friendly compared to traditional halogen additives. Wang et al. reported that the presence of phosphazene derivative enhanced flame retardancy of epoxy resin (EP) [133]. Hexachlorocyclotriphosphazene (HCCP) is one common cyclophosphane precursor reported by Wang [133]. Compared to neat EP, cyclophosphane/EP system containing about 10% of the additive can produce residue weight fraction between 6 and 24% when heated in nitrogen atmosphere, as shown in Figure 9. The char retention increases with increasing cyclophosphazene wt.%, in both nitrogen and air atmospheres. Scanning electron microscopic analysis of the char formed showed that the cyclophosphazene/epoxy resin (EP) char has a more compact and dense structure than that for the neat EP [133].

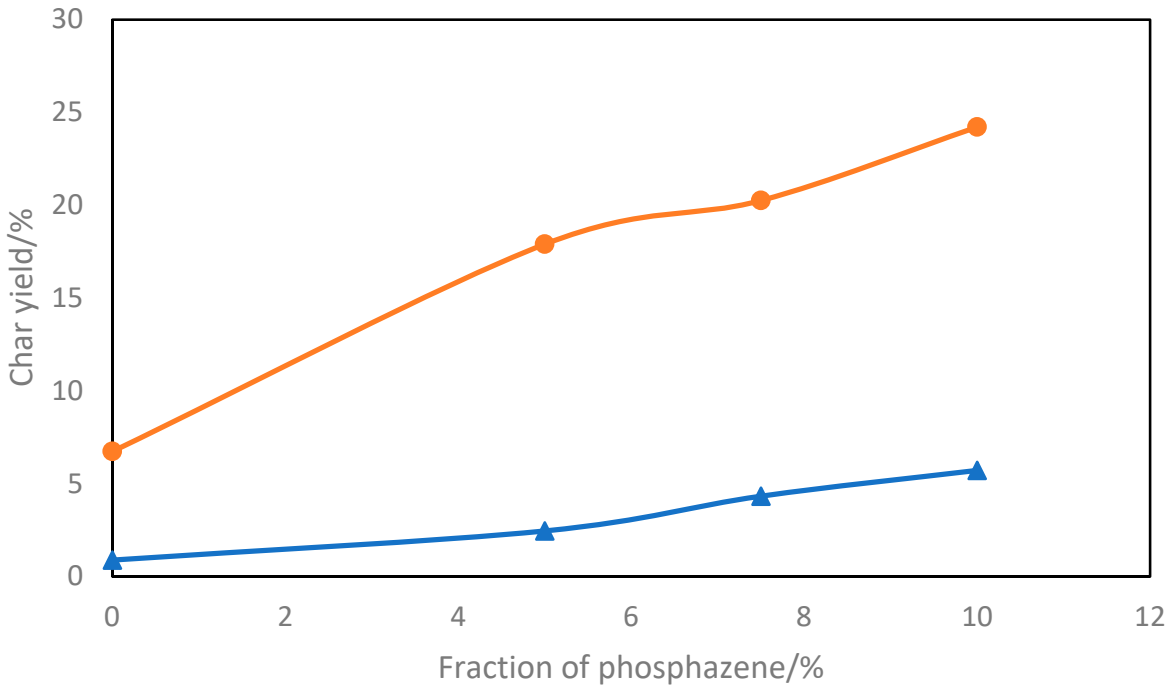

Figure 9. Effect of phosphazene weight fraction on the char yield for epoxy/phosphazene composites, in nitrogen (●) and air (▲) atmosphere [133].

Also, like other phosphorus-based fire retardants, phosphazene is believed to release radicals into the gas phase to inhibit combustion. Rangaraj et al. reported that phosphazene/polypropylene blend produced enhanced thermal properties [134]. In their work, Rangaraj and his co-workers used the HCCP as the precursor material. HCCP was pre-treated with bisphenol-S and aminopropyltrimethoxysilane in order to obtain amine-functionalized phosphazene. Then coupling between modified phosphazene and polypropylene-graft-maleic anhydride (PP-g-MA) was carried out to obtain polypropylene-phosphazene composites. X-ray photoelectron spectroscopy (XPS) was used to perform elemental analysis. Thermal stability and limiting oxygen index (LOI) were found to increase after the introduction of phosphazene as shown in Figure 10. LOI was calculated by using the Van Krevelen equation (Equation (5)) [135]. Both the char yield and LOI increased with increasing weight fraction of amine-functionalized phosphazene, APZS (Figure 10). The Young's modulus and impact strength for the PP/PZA composites were found to vary with the weight fraction of phosphazene. The Young's modulus slightly increased with addition of phosphazene until weight fraction of about 5 wt.% after which it slightly decreased until it reaches about 10 wt.% loading. As for impact strength, the impact strength for PP/PZA composite was higher than that for neat PP at low weight fraction of PZA. However, once weight fraction of PZA exceeds 10 wt.%, the impact strength of the composite begins to decrease. The limited oxygen index (LOI) was calculated from Equation (3) by using the char yield obtained during pyrolysis in nitrogen atmosphere. Accordingly, increasing char yield results in increasing LOI.

$$LOI = 17.5 + 0.4 \times cy. \quad (5)$$

where *cy* indicates the % char yield of the sample.

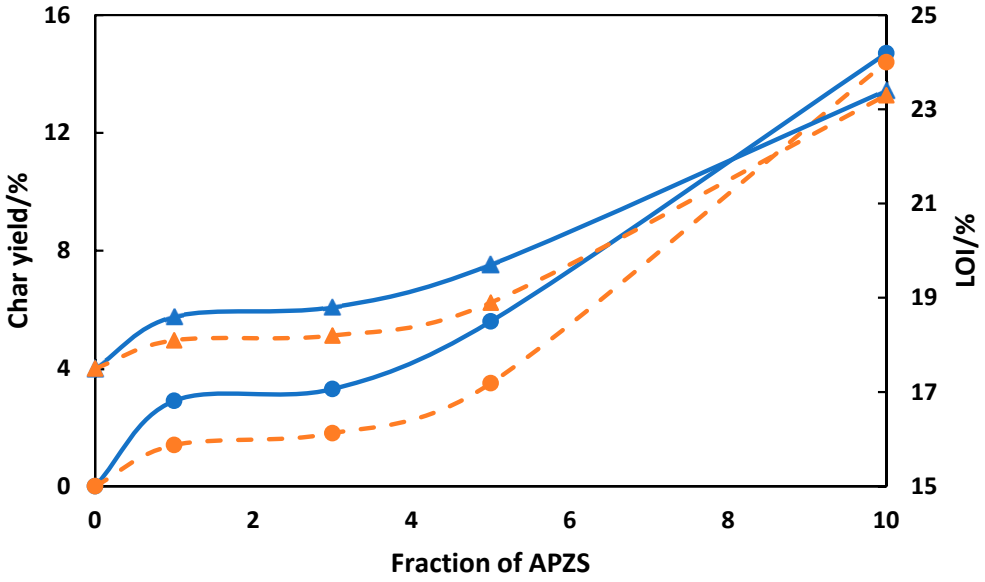

Figure 10. Thermal stability and flame retardancy of PP/phosphazene composites as a function of phosphazene concentration: Char yield (●) and LOI (▲) in air (dash orange) and nitrogen (solid blue) atmosphere [134].

The chemically modified amine-functionalized phosphazene can be used as comonomer for copolymerization in order to significantly enhance the thermal properties of polymer. Kumar et al. synthesized a polyimide-co-phosphazene copolymer by using diamine terminated cyclophosphazene as the comonomer. 2,2′-dioxybiphenylyl substitution was used to form a diamine terminated phosphazene which was then coupled with the dianhydride monomer to obtain phosphazene modified polyimide shown in Scheme 4 [136]. Unlike the commercial linear polyimide, the char yield in air atmosphere for the phosphazene-co-polyimide copolymer is notably high. The char yield of modified polyimide ranges from 50–58% in air atmosphere. Kumar et al. pointed out that the presence of high percentage of phosphorus in phosphazene ring can provide a reasonable explanation for high char yield. In Figure 11, a comparison of thermal decomposition behavior in air for neat PI, neat phosphazene, PI-PDMS [57] and PI-co-phosphazene [136] is shown. Neat polyimide and hexachlorophosphazene decomposed almost completely in air, like most carbon-based polymers. The presence of linear PDMS blocks in the backbone of PDMS-block-PI increases the char yield up to 10%. The enhancement of fire retardancy for phosphazene-co-polyimide due to the attachment of phosphazene unit in the co-polyimide backbone is remarkable and results in the formation of much higher char yield in air of ≥50%.

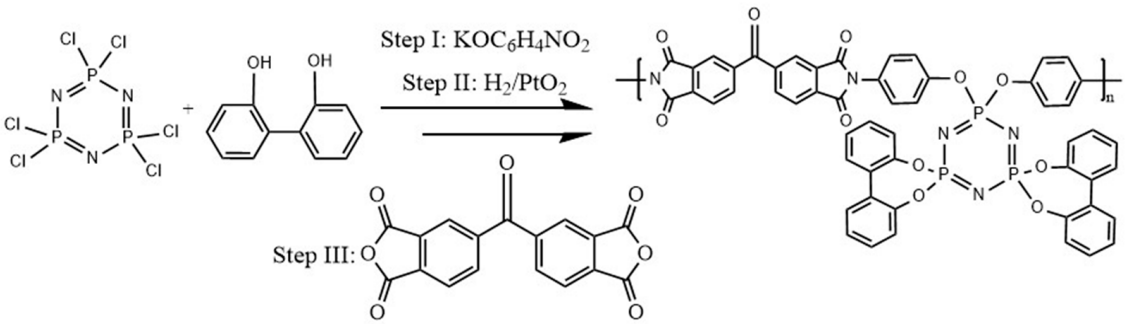

Scheme 4. Schematic representation of the synthesis of polyimide copolymer containing amine-functionalized phosphazene [136].

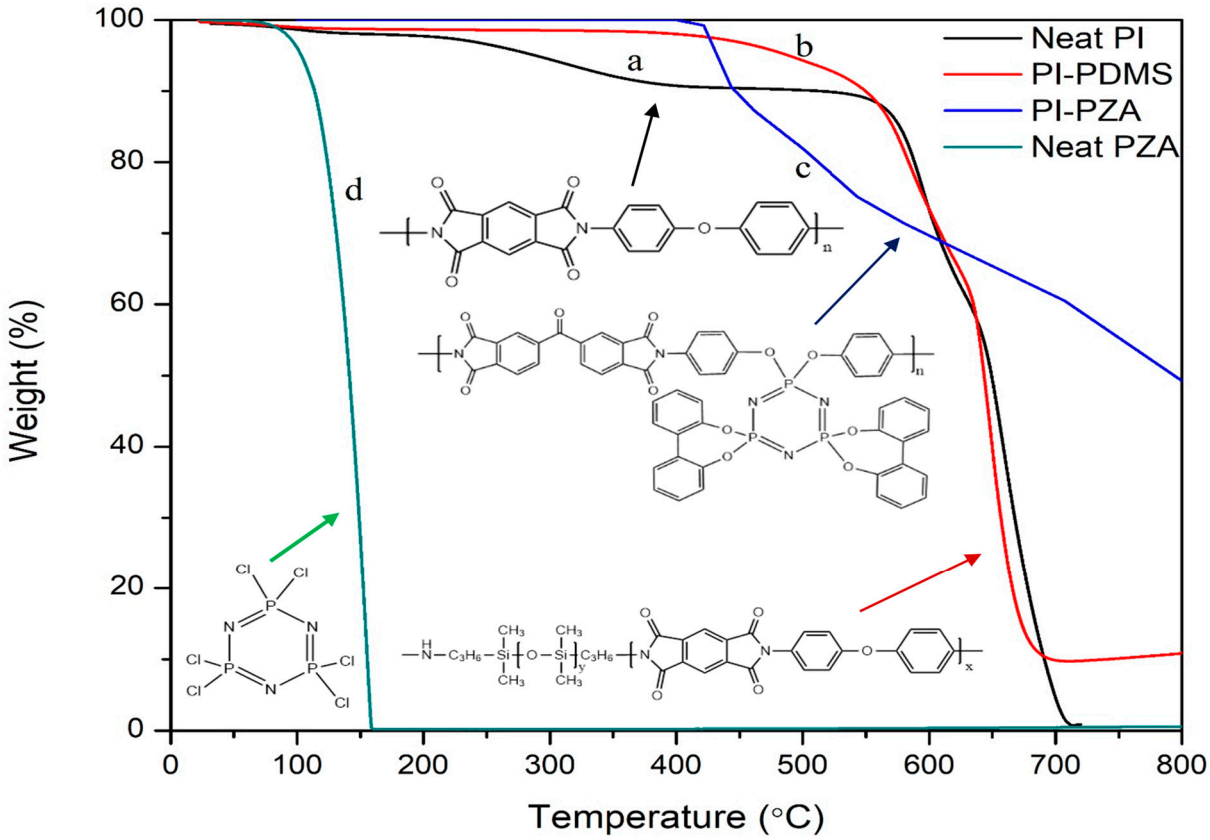

Figure 11. TGA traces of (a) neat polyimide, (b) PI-PDMS block copolymer, (c) PI-Phosphazene copolymer, and (d) neat phosphazene in air atmosphere [57,136].

It should be noted that the presence of chloride group in phosphazene may lead to undesirable environmental issues. The alternative is to use commercial grade cyclotriphosphazene derivatives. There are serval reports about the flame retardancy of phosphazene derivatives [137,138]. For instance, aziridinyl phosphazene, which is shown in Scheme 5, can be considered as one candidate. Aziridine ring can behave in a way similar to the epoxy ring. It can undergo ring-opening reaction just like the oxirane ring as shown in Scheme 6. This reaction tends to occur when the side substituents of aziridine (R) are electron-withdrawing and strong nucleophiles, such as amines.

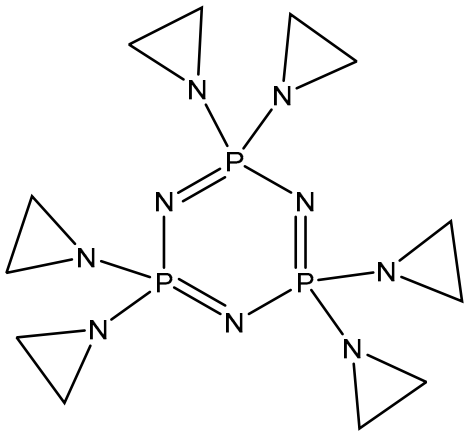

Scheme 5. Structure of aziridinyl phosphazene.

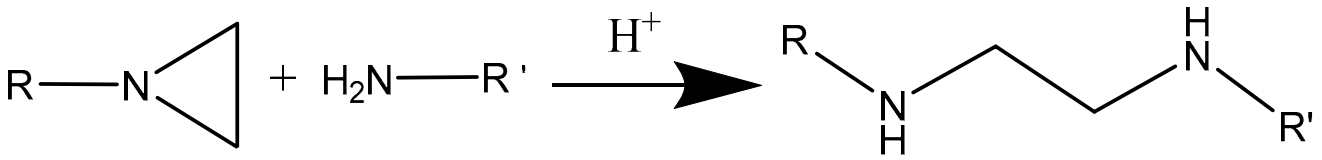

Scheme 6. Ring-opening reaction of aziridine with amine.

5. Silicone-Based Flame Retardants

Silicone-based additives are another promising class of flame-retardant additives [139–144]. The dissociation energy of Si-O bond is 108 kcal/mol which is higher than 85.2 kcal/mol for C-C bonds or 82.6 kcal/mol for C-O bonds [51]. This very fundamental property ensures greater thermal resistance for silicone-based materials compared to traditional organic carbon-carbon compounds. Si-O bond can serve as oxygen sink during thermal oxidation and can transform itself into silica, SiO_2. Other silicon based covalent bonds such as Si-Si and Si-N bonds show similar mechanism but with better performance because they can consume more oxygen atoms.

There are plenty of choices among the silicone-based compounds that are flame retardants. The mechanism and addition methods are also varied. The thermal behavior of silicone is dependent on its structure. Polysiloxanes with silanol end group (Si-OH) would decompose by unzipping mechanism [145]. Polysiloxanes without such end-capped functional groups have different mechanism. Inter or intra molecular redistribution occur randomly between siloxane backbones. This thermal degradation mechanism will result in the formation of cyclic oligomers and silica. Such mechanism is called random scission reaction. Moreover, there is one more case of thermal degradation for polysiloxanes. Some polar impurities and additives in polysiloxanes would lead to externally catalyzed degradation. The Si-O backbone will hydrolyze in the presence of polar impurities.

The fire retardancy of silicones-based materials show both mechanisms. Many reports show that thermally stable residues and silica are formed under high-temperature treatment. The heating rate mainly decides the fraction of residues [146]. For instance, at slow heating rate, cyclic oligomers would be the main product. On the other hand, increasing heating rate creates more tetramer. Radicals are also formed during bonds scission. The production of radicals can only occur at high temperature, leading to the release of methane and macro radicals. Coupling between radicals would strongly decrease the flexibility of polysiloxanes and slow down the degradation of oligomers. One important advantage of most silicone-based fire retardants is that the combustion of silicone-based materials produces little or no toxic gasses. The possible pathways of thermal oxidation of silicone-based materials are shown in Figure 12 [146].

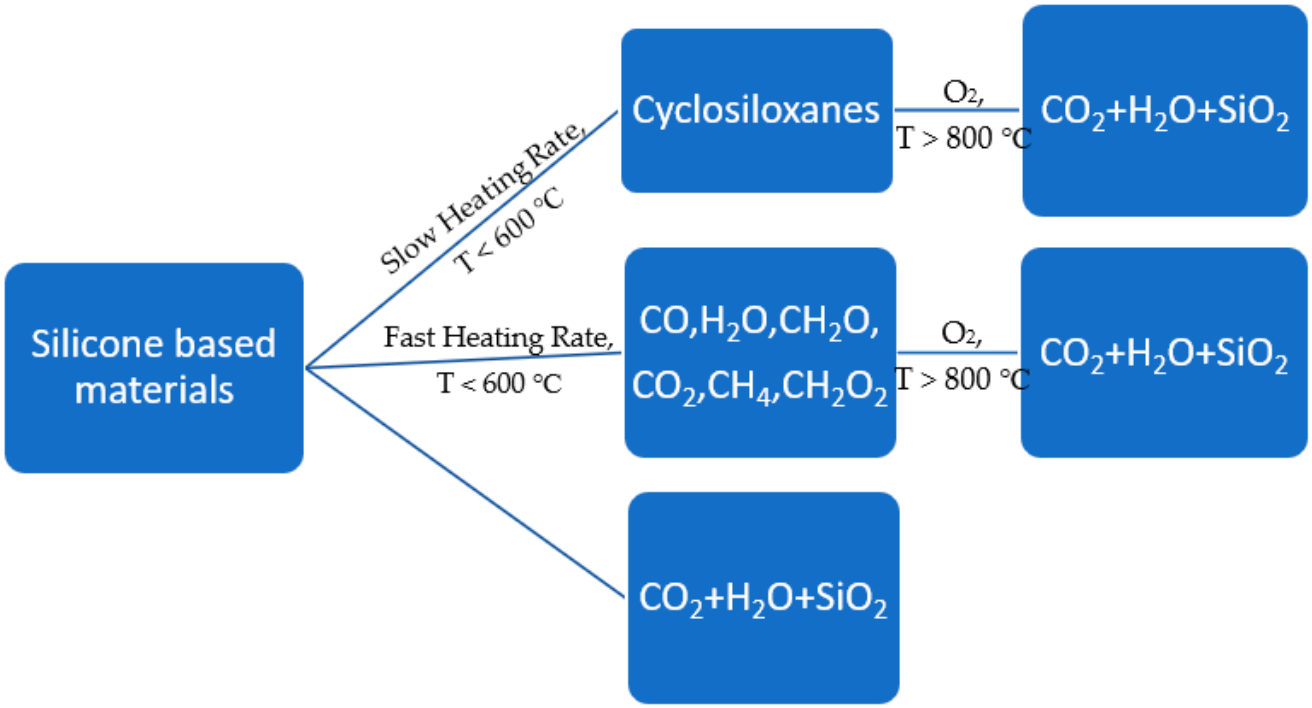

Figure 12. Representation of the products of thermal oxidation of silicone-based materials under different conditions [146].

Flame retardancy can be affected by the structures of silicone-based materials, like other aspects of performance, including the end-group, side-group, and polymer main chain. As was discussed above, the end-group affects the thermal decomposition mechanism of PDMS. Methyl end-groups provide better thermal stability for PDMS than hydroxyl terminated structures [147]. When vinyl groups are added to the system, the thermal stability would be lower than that for methyl terminated PDMS. Also, the nature of the side group has influence on polysiloxanes decomposition. It was reported that methyl side group structure is more stable than Si-H side group [148]. The thermal stability of polysiloxanes can be enhanced if phenyl groups were incorporated into the chain. PDMS is naturally stable in neutral environment around 340 °C. In the presence of small amount of methylphenylsiloxane or diphenylsiloxane, the onset degradation temperature would be increased to about 400 °C [149]. The effect of molecular weight is also to be noted. Based on published reports, longer siloxane chain would give shorter ignition time in cone calorimetry [150]. The reason of this effect is that the length of chain decides the amount of combustible hydrocarbon in system. On the other hand, the mass of residues is proportional to the molecular weight of polysiloxanes.

Silicone elastomeric nanoparticles (S-ENP) prepared by spray drying the silicone latex was physically mixed with Nylon-6 in an extruder followed by extrusion as was reported by Dong et al. [151]. In cone calorimeter tests, modified nylon composites show better flame retardancy than neat nylon 6 shown in Table 1. With incorporation of exfoliated clay, the flame retardancy of the system can be further enhanced. An improved flame retardancy has been confirmed based on observation of the combustion residues [96].

Silica/polyimides nanocomposite aerogel was reported 2020 by Zhang et al. [152]. Aerogels are well-known as outstanding thermal isolation due to high porosity and low density [153]. A novel co-gel preparation strategy was highlighted here to obtain the hierarchically porous structure of aerogels. The LOI of PI/silica composites could be raised up to 48 compared to neat PI with 34 for LOI.

Table 1. Dependence of Peak HRR and Time to Peak HRR on composition for nylon-6 and PA/clay/silicone nanocomposites (heat flux of 35 kW/m^2) [153].

Samples	Peak HRR (kW/m^2)	Time to Peak HRR (s)	Mean HRR (kW/m^2)
Nylon-6	790	375	370
PA-1 [a]	317	685	129
PA-2 [b]	249	380	110

[a]: 10 wt.% of S-ENP, [b]: 10 wt.% S-ENPC(S-ENP/clay (4/1)).

Polyhedral Oligomeric Silsesquioxanes (POSS)

Nanoparticles are now attracting lots of attention in materials engineering. Organic-inorganic composite materials are believed to lead to revolution of high-performance materials. Combination of inorganic components and polymers could provide enhancements of both high rigidity due to the inorganic materials and flexibility of polymer [154–158].

POSS was first reported by Scott in 1946 [159]. It is regarded as one of the smallest silica nanoparticles with diameters of 1–3 nm [160,161]. The empirical formula of Silsesquioxanes is $RSiO_{1.5}$, where R can be a hydrogen atom or different group such as alkyl, alkylene, or acrylate. A wide range of options for the end-groups can be achieved by chemical modification. Structures of silsesquioxanes can be found in different shapes as shown in Figure 13, where R represents a functional group, such as hydroxyl and amine.

POSS has inherent high thermal resistance and excellent mechanical properties [162–171]. For instance, Handke et al. reported that ladder-like polysilsesquioxanes decompose at temperatures >400 °C [172]. Highly crosslinked POSS produces about 70% residues under nitrogen pyrolysis. Some researchers reported that incorporation of polysiloxane blocks into carbon-based polymer might severely decrease the flexibility of polymers [173]. POSS-based copolymers can overcome this flaw and effectively enhance mechanical and thermal properties. Feng et al. reported that the char yield of PI increased in the presence of increasing amount of ladder-like POSS [174].

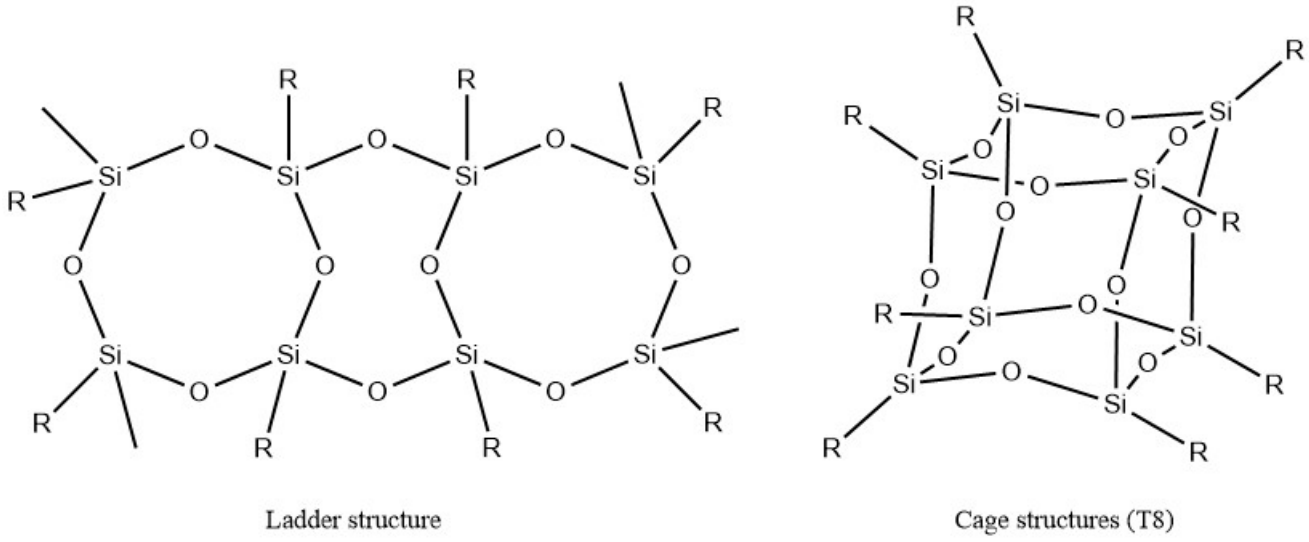

Figure 13. Schematic representation of Silsesquioxanes [165].

Fan et al. has reported a crosslinked polyimide with functionalized cage POSS as crosslinker [175,176]. The improvement of thermal properties of PI was confirmed by DSC and TGA tests, including increase in the T_g and thermal stability. The most significant outcome is the LOI increase from 46.5% for neat PI to 57% with 5.43 wt.% of POSS.

6. Hybrid Systems

To achieve optimal flame retardancy, a combination of multiple flame-retardant additives must be considered. One important advantage of a hybrid system is that flame retardancy can be achieved in several ways or different mechanisms. Hence, high efficiency of fire retardancy can be achieved [177–191].

In 2019, Revathi et al. reported a nanocomposite of phosphazene core-base POSS-reinforced polyimide materials [192]. The hybrid composite was synthesized by coupling of phosphazene to naphthalene tetracarboxylic dianhydride (NTDA) to form phosphazene imide (PZI) copolymer. Additionally, a cage shaped POSS with amino ended group was then reacted with PZI copolymer to complete the last puzzle and form the hybrid system [192] as shown in Scheme 7).

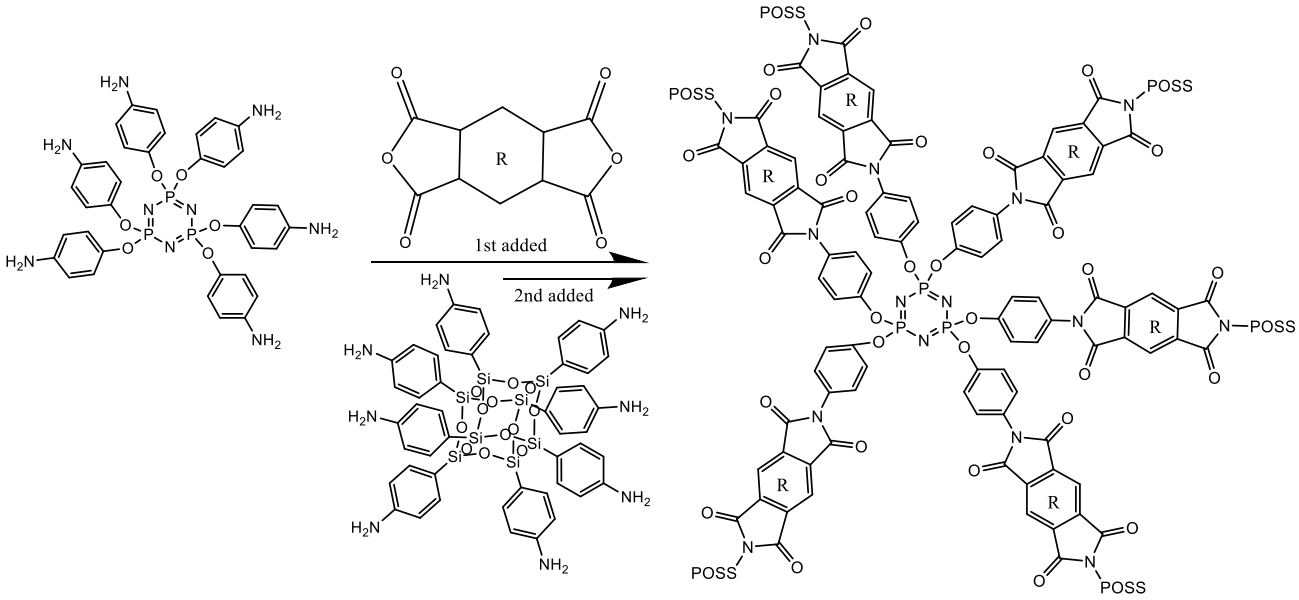

Scheme 7. Representation of the structure of phosphazene core based POSS reinforced polyimide [192].

This POSS-PZI nanocomposite was evaluated for different properties. TGA analysis shows that POSS/PZI composite containing 10 wt.% POSS has 14% higher char yield in nitrogen atmosphere at 800 °C than neat PZI as shown in Figure 14. LOI calculated by using Krevelen equation [135], shows that that the LOI of PZI/POSS composites increased with increasing amount of POSS. The glass transition temperature of POSS-PZI obtained by differential scanning calorimetry, DSC, shows increased T_g of PZI/POSS with increasing amount of POSS, from 238 °C for neat PZI to 297 °C for PZI/POSS containing 10 wt.% of POSS. The LOI of POSS-PZI composites were also higher than that for neat PZI. It increased from 39.9% for neat PZI to 45.5% for PZI/POSS containing 10% POSS. This paper also reported that anti-bacterial effect and UV shielding behavior were also improved with addition of POSS. However, this system can be improved further. First, the comparison was only done for PZI and PZI-POSS composites. The role of phosphazene was not fully understood. Secondly, the polyimide studied in this work was synthesized by using amino terminated phosphazene and naphthalene tetracarboxylic dianhydride, NTDA. This would create a highly crosslinked structure and shorter linear polymer chain. Such a system might strongly decrease the mechanical properties and processability for ultra-high stiffness of chains. Hence, significant improvements and modifications can be made.

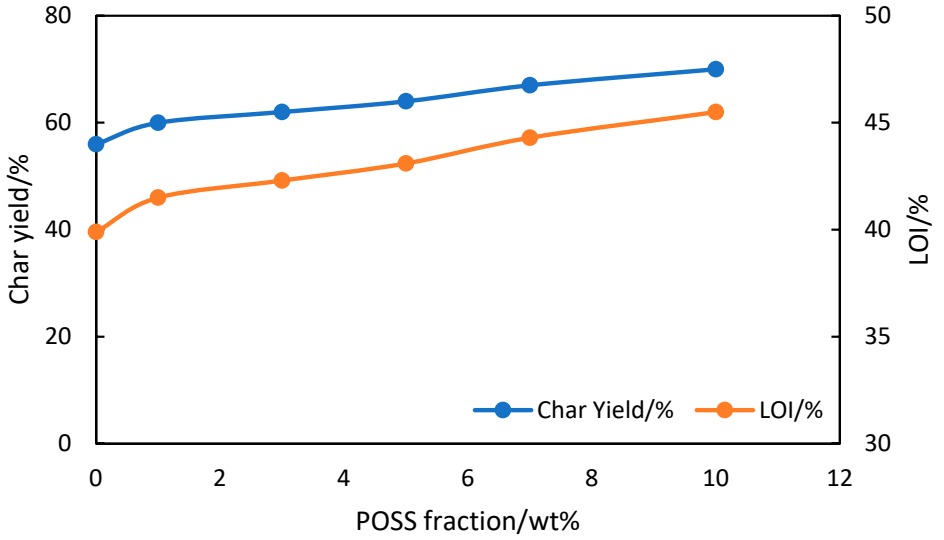

Figure 14. Dependence of char yield and LOI for phosphazene/POSS polyimide composites on wt.% POSS [192].

7. Comparison of Techniques Used for Flame Retardancy

In this section, serval important techniques that are used to measure decomposition and flammability behavior of polyimide and polyimide nanocomposites are reviewed. A brief compassion of these techniques is shown in Table 2.

Table 2. Comparison of commonly used flame-retardancy techniques.

	TGA	DSC	LOI/UL-94
Sample Scale	mg	mg	g
Strength	Monitor weight change under controllable heat conditions. Char yield, T_d, LOI	Calorimeter method, measuring phase transition (T_g, T_m) temperature, heat capacity and enthalpy change	Commercially preferred standard flame-retardant test, easy, and low-cost
Weakness	Lack of information on heat release	Usually test under T_d, cannot provide weight-loss conditions	Insufficient sensitivity
	Cone Calorimeter		**MCC**
Sample Scale	g		mg
Strength	Provide detailed information on combustion, including mass loss, heat-release rate (HRR), total heat released (THR), time to ignition, and time of combustion/extinction		Non-flaming combustion methods separately control and study the pyrolysis and thermal oxidation
Weakness	Require large scale and specific dimension samples		Accuracy influenced by potential side products of decomposition, such as water vapor and carbon oxide

(T_d: Degradation temperature, T_g: Glass transition temperature, and T_m: Melting temperature).

Thermal gravimetric analysis (TGA) is a fundamental tool for thermal properties study. TGA can measure the mass change of samples under programmed and controlled heating procedure. The weight change caused by breakage of covalent bonds and loss of small molecule, such as water, can be monitored. By comparing the weight of residues which is regarded as char yield (Cy) and degradation temperature (T_d), the thermal stability of a material can be determined. Also, the derivative weight-loss analysis based on the integral of the area under the derivative weight-loss curve is used to calculate the decomposition rate of materials. TGA analysis can be done under different gaseous atmosphere, including inert nitrogen atmosphere and oxidizing oxygen or air atmosphere. By means of the Kissinger–Akahira–Sunose (KAS) model (shown in Equation (6)), the activation energy of the respective thermal process can be determined from the TGA data obtained at a handful of heating rates. The activation energy for decomposition is usually obtained from the slope of $\ln\beta/T^2$ vs. $1/T$ where β is the heating rate [193]. Besides, there are two other methods which can be used to evaluate the decomposition processes, including the Friedman method (Equation (7)) and the Ozawa–Flynn–Wall method (Equation (8)) [194–197]. TGA char retention data can also be used to estimate the limiting oxygen index (LOI) from the Van Krevelen equation (Equation (5)).

$$\ln\frac{\beta}{T^2} = \ln\left(\frac{AR}{E_a g(\alpha)}\right) - \frac{E_a}{RT} \tag{6}$$

where α is the degree of conversion, β is the heating rate, $g(\alpha)$ is the integral conversion function, A is the pre-exponential factor, R is the gas constant, and Ea is the activation energy.

$$\ln\frac{d\alpha}{dt} = \ln\beta\frac{d\alpha}{dT} = \ln[Af(\alpha)] - \frac{E}{RT}. \tag{7}$$

where the E is the activation energy, A is the pre-exponential factor (s^{-1}), and $f(\alpha)$ is the conversion function. In the Friedman method, ln dα/dt vs. $1/T$ is plotted for different heating rates. A straight line is drawn through the same α value for the thermogram with different heating rates. The activation energy is then obtained from the slope of this isoconversional line.

$$G(\alpha) = \frac{A}{\beta}\int_{T_0}^{T_p} e^{-\frac{E}{RT}}dT = \int_0^{\alpha_p}\frac{d\alpha}{f(\alpha)}. \tag{8}$$

where T_0 is the initial temperature (when α = 0), and T_p is the peak temperature in DTG curves. The Ozawa–Flynn–Wall method extracts the activation from the slope of the linear line of $\ln\beta$ vs. $1/T$ curve.

The differential scanning calorimetry, DSC is another important analytical technique used to determine heat of thermal transitions and thermal transition temperatures. It is also used to determine the heat of reaction as well as the heat of decomposition. In DSC, the heat change due to state/phase transition is measured. The glass transition temperature (T_g), crystallization temperature, T_c and the melting temperature, T_m can be determined by DSC. To avoid the influence of thermal oxidation and other chemical reaction such as thermal degradation, the temperature range for DSC test is usually set to be lower than decomposition starting point and samples are tested under inert atmosphere, such as nitrogen or argon atmosphere. When DSC is carried out at high temperatures $\geq$ 400 °C and under an oxidizing atmosphere, the heat of decomposition and the heat capacity of decomposition can be determined.

There are three commonly used techniques for flammability tests of materials: UL-94 test, limiting oxygen index (LOI) test, and calorimeter test. All these three techniques can provide quantitative information about how flammable a material is [198–206]. For LOI test, the minimum concentration of oxygen in an oxygen–nitrogen mixture atmosphere needed for materials combustion is measured. However, recent study has indicated that LOI test has some limitations. Extinguishing of flame might occur because of the dripping of materials that might take the flame away from combustion zone, thereby giving a higher LOI values

than expected. Also, some researchers pointed out that LOI might unexpectedly vary with the concentration of flame retardant. In some cases, LOI might decrease after reaching the peak of effectiveness along with the addition of flame retardant [207]. Therefore, an empirical calibration curve is required for this system. As for UL-94 test, it is widely applied in both industry and academia. The materials are ignited by a controlled burner in UL-94. The after-flame time, which is the time required for the flame to extinguish, is recorded. To ensure the accuracy, cohesive samples are generally preferred to avoid potential error created by samples flowing.

Calorimetry in the form of Cone calorimetry, or Microscale combustion calorimetry, MCC is capable of providing more quantitative parameters including the heat-release rate (HRR), total heat of combustion, and onset temperature for combustion, making it reliable in measuring flame retardancy. In cone calorimeter test, a forced combustion of organic sample is accomplished by projected radiant heat [208,209]. The heat-release rate, time to ignition (TTI), total heat release (THR), and mass-loss rate are monitored by using a series of sensors. The heat of combustion (h_c) can be calculated by using Equation (9).

Recently, microscale combustion calorimeter (MCC) has gained lots of attention. One commonly known advantage of MCC, is that it consumes less energy and small amount of samples, usually in the milligram scale, which makes it more preferable and adaptable. MCC can simulate the combustion condition based on a different mechanism as cone calorimeter [210–215]. In contrast to real flaming tests, MCC creates a well-controlled premixed burning which can sustain the pyrolysis and combustion (oxidation of volatile fuel) separately. On the contrary, flaming combustion faces the huddle of controlling of the entire process which might lead to insufficient combustion. The most important part in MCC set-up is a pyrolysis-combustion flow calorimeter which consists of individually controlled reactors of fuel generation and heat generation. This arrangement makes it possible to alter the heating conditions and composition of atmosphere in condensed phase and gaseous phase separately.

$$h_c = \frac{THR}{1 - Cy} \tag{9}$$

8. Conclusions

This review is focused primarily on flame-retardant behavior of polyimides, an engineering high-temperature polymer, and its composites and copolymers. The synergetic fire-retardancy effect of the polyimide and its copolymers and commonly used flame-retardant additives is described. Because polyimide is considered as a potential candidate for dielectric and energy storage application, the potential for fire hazard must be a concern as is the case with all carbon-based materials. Because of the presence of aromatic phenyl ring in its backbone, polyimide can serve as a fire retardant in the condensed phase by forming protective char layer during pyrolysis. Neat polyimide can produce about 55% char yield when heated under inert atmosphere, however, combustion of PI in air leads to catastrophic failure. Hence, the flame retardancy of polyimide could be improved by introducing materials such as POSS and phosphazene to improve its flame retardancy in oxidizing and inert atmospheres. Carbon-based nano composites like carbon nanotubes and graphene can improve char yield. When reinforced with graphene, the composites char failure rate is 40% lower than that for neat polyimide. Silicone base nanoparticles such as POSS can also enhance the flame retardancy in both the condensed and gaseous phases and the product of its pyrolysis is ultra-thermally stable. The heat-release rate of silicone nanoparticles incorporated into polyimide is about 60% lower than that for the neat polyimide. Phosphorus-based fire retardants can release radical into the gaseous phase, which couples with flammable radical to form inactive species in the gaseous phase. For a polyimide copolymer containing phosphazene in the backbone, the char yield in air atmosphere is as high as 50%. A combination of polyimide matrix and other flame retardants can provide a new paradigm for design and construction of smart fire retardants capable of dual mechanism of fire retardancy while maintaining high thermomechanical

properties. A phosphazene core-based POSS-PI copolymer was reported to show increased char yield with increasing amount of POSS. However, the effect of POSS on the processability and mechanical performance of the copolymer is not fully understood and needs to be determined.

Author Contributions: S.X. (data curation and analysis), C.A. and J.L. (Data curation), J.O.I. (Original concept, organization, administration, data analysis). All authors have read and agreed to the published version of the manuscript.

Funding: This research received no external funding.

Institutional Review Board Statement: Not applicable.

Informed Consent Statement: Not applicable.

Data Availability Statement: As per the cited articles.

Conflicts of Interest: The authors declare no conflict of interest.

References

1. Laoutid, F.; Bonnaud, L.; Alexandre, M.; Lopez-cuesta, J.; Dubois, P. New Prospects in Flame Retardant Polymer Materials: From Fundamentals to Nanocomposites. *Mater. Sci. Eng. R Rep.* **2009**, *63*, 100–125. [CrossRef]
2. Camino, B.; Camino, G. The Chemical Kinetics of the Polymer Combustion Allows for Inherent Fire Retardant Synergism. *Polym. Degrad. Stab.* **2019**, *160*, 142–147. [CrossRef]
3. Emmons, H.W.; Atreya, A. The Science of Wood Combustion. *Proc. Indian Acad. Sci. Sect. C Eng. Sci.* **1982**, *5*, 259–268.
4. Elbasuney, S. Novel Multi-Component Flame Retardant System Based on Nanoscopic Aluminium-Trihydroxide (ATH). *Powder Technol.* **2017**, *305*, 538–545. [CrossRef]
5. Zhang, X.; Guo, F.; Chen, J.; Wang, G.; Liu, H. Investigation of Interfacial Modification for Flame Retardant Ethylene Vinyl Acetate Copolymer/Alumina Trihydrate Nanocomposites. *Polym. Degrad. Stab.* **2005**, *87*, 411–418. [CrossRef]
6. Zanetti, M.; Camino, G.; Canavese, D.; Morgan, A.B.; Lamelas, F.J.; Wilkie, C.A. Fire Retardant Halogen-Antimony-Clay Synergism in Polypropylene Layered Silicate Nanocomposites. *Chem. Mater.* **2002**, *14*, 189–193. [CrossRef]
7. Wu, G.M.; Schartel, B.; Bahr, H.; Kleemeier, M.; Yu, D.; Hartwig, A. Experimental and Quantitative Assessment of Flame Retardancy by the Shielding Effect in Layered Silicate Epoxy Nanocomposites. *Combust. Flame* **2012**, *159*, 3616–3623. [CrossRef]
8. Chen, Y.; Iroh, J.O. Synthesis and Characterization of Polyimide/Silica Hybrid Composites. *Chem. Mater.* **1999**, *11*, 1218–1222. [CrossRef]
9. Feng, L.; Iroh, J.O. Corrosion Resistance and Lifetime of Polyimide-b-Polyurea Novel Copolymer Coatings. *Prog. Org. Coat.* **2014**, *77*, 590–599. [CrossRef]
10. Feng, L.; Iroh, J.O. Polyimide–Polyurea Copolymer Coating with Outstanding Corrosion Inhibition Properties. *J. Appl. Polym. Sci.* **2018**, *135*, 45861. [CrossRef]
11. Sezer Hicyilmaz, A.; Celik Bedeloglu, A. Applications of Polyimide Coatings: A Review. *SN Appl. Sci.* **2021**, *3*, 363. [CrossRef]
12. Marashdeh, W.; Iroh, J.O. Electrical Properties of Flexible Graphene Reinforced Polyimide Composites. *J. Appl. Polym. Sci.* **2017**, *134*, 6–11. [CrossRef]
13. Feng, L.; Iroh, J.O. Polyimide- b -Polysiloxane Copolymers: Synthesis and Properties. *J. Inorg. Organomet. Polym. Mater.* **2013**, *23*, 477–488. [CrossRef]
14. Maier, G. Low Dielectric Constant Polymers for Microelectronics. *Prog. Polym. Sci.* **2001**, *26*, 3–65. [CrossRef]
15. Chisca, S.; Musteata, V.E.; Sava, I.; Bruma, M. Dielectric Behavior of Some Aromatic Polyimide Films. *Eur. Polym. J.* **2011**, *47*, 1186–1197. [CrossRef]
16. Hendricks, N. Organic Polymers for IC Intermetal Dielectric Applications. *Solid State Technol.* **1995**, *38*, 117.
17. Okafor, P.A.; Huxel, B.; Iroh, J.O. Electrochemical Behavior of Multifunctional Graphene-Polyimide Nanocomposite Film in Two Different Electrolyte Solutions. *J. Appl. Polym. Sci.* **2015**, *132*, 42673. [CrossRef]
18. Okafor, P.; Iroh, J. Electrochemical Properties of Porous Graphene/Polyimide-Nickel Oxide Hybrid Composite Electrode Material. *Energies* **2021**, *14*, 582. [CrossRef]
19. Banerjee, S.; Madhra, M.K.; Salunke, A.K.; Maier, G. Synthesis and Properties of Fluorinated Polyimides. 1. Derived from Novel 4,4″-Bis(Aminophenoxy)-3,3″-Trifluoromethyl Terphenyl. *J. Polym. Sci. Part A Polym. Chem.* **2002**, *40*, 1016–1027. [CrossRef]
20. Fitzgerald, J.J.; Tunney, S.E.; Landry, M.R. Synthesis and Characterization of a Fluorinated Poly (Imide-Siloxane) Copolymer: A Study of Physical Properties and Morphology. *Polymer* **1993**, *34*, 1823–1832. [CrossRef]
21. Ye, Y.-S.; Chen, W.-Y.; Wang, Y. Synthesis and Properties of Low-Dielectric-Constant Polyimides with Introduced Reactive Fluorine Polyhedral Oligomeric Silsesquioxanesle. *J. Polym. Sci. Part A Polym. Chem.* **2006**, *44*, 5391–5402. [CrossRef]
22. Chung, I.S.; Park, C.E.; Ree, M.; Kim, S.Y. Soluble Polyimides Containing Benzimidazole Rings for Interlevel Dielectrics. *Chem. Mater.* **2001**, *13*, 2801–2806. [CrossRef]

23. Stoakley, D.M.; St. Clair, A.K.; Croall, C.I. Low Dielectric, Fluorinated Polyimide Copolymers. *J. Appl. Polym. Sci.* **1994**, *51*, 1479–1483. [CrossRef]
24. Carter, K.R.; DiPietro, R.A.; Sanchez, M.I.; Swanson, S.A. Nanoporous Polyimides Derived from Highly Fluorinated Polyimide/Poly(Propylene Oxide) Copolymers. *Chem. Mater.* **2001**, *13*, 213–221. [CrossRef]
25. Park, S.J.; Cho, K.S.; Kim, S.H. A Study on Dielectric Characteristics of Fluorinated Polyimide Thin Film. *J. Colloid Interface Sci.* **2004**, *272*, 384–390. [CrossRef] [PubMed]
26. Luo, X.; Lu, X.; Chen, X.; Chen, Y.; Song, C.; Yu, C.; Wang, N.; Su, D.; Wang, C.; Gao, X.; et al. A Robust Flame Retardant Fluorinated Polyimide Nanofiber Separator for High-Temperature Lithium–Sulfur Batteries. *J. Mater. Chem. A* **2020**, *8*, 14788–14798. [CrossRef]
27. Chen, Y.; Kang, E.T. New Approach to Nanocomposites of Polyimides Containing Polyhedral Oligomeric Silsesquioxane for Dielectric Applications. *Mater. Lett.* **2004**, *58*, 3716–3719. [CrossRef]
28. Marashdeh, W.F.; Longun, J.; Iroh, J.O. Relaxation Behavior and Activation Energy of Relaxation for Polyimide and Polyimide-Graphene Nanocomposite. *J. Appl. Polym. Sci.* **2016**, *133*, 43684. [CrossRef]
29. Song, Z.; Zhan, H.; Zhou, Y. Polyimides: Promising Energy-Storage Materials. *Angew. Chem. Int. Ed.* **2010**, *49*, 8444–8448. [CrossRef]
30. Li, Q.; Yao, F.Z.; Liu, Y.; Zhang, G.; Wang, H.; Wang, Q. High-Temperature Dielectric Materials for Electrical Energy Storage. *Annu. Rev. Mater. Res.* **2018**, *48*, 219–243. [CrossRef]
31. Chi, Q.; Gao, Z.; Zhang, T.; Zhang, C.; Zhang, Y.; Chen, Q.; Wang, X.; Lei, Q. Excellent Energy Storage Properties with High-Temperature Stability in Sandwich-Structured Polyimide-Based Composite Films. *ACS Sustain. Chem. Eng.* **2019**, *7*, 748–757. [CrossRef]
32. Williams, D.L.; Electrochem, J.; Williams, D.I.; Byrne, J.J.; Driscoll, J.S. A High Energy Density Lithium/Dichloroisocyanuric Acid Battery System. *J. Electrochem. Soc.* **1969**, *116*, 2–5. [CrossRef]
33. Wang, Y.; Wang, L.; Yuan, Q.; Chen, J.; Niu, Y.; Xu, X.; Cheng, Y.; Yao, B.; Wang, Q.; Wang, H. Ultrahigh Energy Density and Greatly Enhanced Discharged Efficiency of Sandwich-Structured Polymer Nanocomposites with Optimized Spatial Organization. *Nano Energy* **2018**, *44*, 364–370. [CrossRef]
34. Palneedi, H.; Peddigari, M.; Hwang, G.T.; Jeong, D.Y.; Ryu, J. High-Performance Dielectric Ceramic Films for Energy Storage Capacitors: Progress and Outlook. *Adv. Funct. Mater.* **2018**, *28*, 1803665. [CrossRef]
35. Sun, W.; Lu, X.; Jiang, J.; Zhang, X.; Hu, P.; Li, M.; Lin, Y.; Nan, C.W.; Shen, Y. Dielectric and Energy Storage Performances of Polyimide/BaTiO3 Nanocomposites at Elevated Temperatures. *J. Appl. Phys.* **2017**, *121*, 244101. [CrossRef]
36. Ai, D.; Li, H.; Zhou, Y.; Ren, L.; Han, Z.; Yao, B.; Zhou, W.; Zhao, L.; Xu, J.; Wang, Q. Tuning Nanofillers in In Situ Prepared Polyimide Nanocomposites for High-Temperature Capacitive Energy Storage. *Adv. Energy Mater.* **2020**, *10*, 1903881. [CrossRef]
37. Hedrick, J.; Labadie, J.; Russell, T.; Hofer, D.; Wakharker, V. High Temperature Polymer Foams. *Polymer* **1993**, *34*, 4717–4726. [CrossRef]
38. Jewell, R.A. Relative Thermophysical Properties of Some Polyimides. *J. Appl. Polym. Sci.* **1971**, *15*, 1717–1727. [CrossRef]
39. Hatori, H.; Yamada, Y.; Shiraishi, M.; Yoshihara, M.; Kimura, T. The Mechanism of Polyimide Pyrolysis in the Early Stage. *Carbon* **1996**, *34*, 201–208. [CrossRef]
40. Sun, G.; Liu, L.; Wang, J.; Wang, H.; Xie, Z.; Han, S. Enhanced Polyimide Proportion Effects on Fire Behavior of Isocyanate-Based Polyimide Foams by Refilled Aromatic Dianhydride Method. *Polym. Degrad. Stab.* **2014**, *110*, 1–12. [CrossRef]
41. Chen, M.; Liang, B.; Guo, Y.; Li, C.; He, X.; Hu, J.; Li, R.; Zeng, K.; Yang, G. Pyrolysis Mechanism of Polyimide Containing Bio-Molecule Adenine Building Block. *Polym. Degrad. Stab.* **2020**, *175*, 109124. [CrossRef]
42. Gu, W.; Wang, G.; Zhou, M.; Zhang, T.; Ji, G. Polyimide-Based Foams: Fabrication and Multifunctional Applications. *ACS Appl. Mater. Interfaces* **2020**, *12*, 48246–48258. [CrossRef] [PubMed]
43. He, L.; Chen, T.; Zhang, Y.; Hu, L.; Wang, T.; Han, R.; He, J.-L.; Luo, W.; Liu, Z.-G.; Deng, J.-N.; et al. Imide-DOPO Derivative Endows Epoxy Resin with Excellent Flame Retardancy and Fluorescence without Losing Glass Transition Temperature. *Compos. Part B Eng.* **2022**, *230*, 109553. [CrossRef]
44. Liu, B.W.; Zhao, H.B.; Chen, L.; Chen, L.; Wang, X.L.; Wang, Y.Z. Eco-Friendly Synergistic Cross-Linking Flame-Retardant Strategy with Smoke and Melt-Dripping Suppression for Condensation Polymers. *Compos. Part B Eng.* **2021**, *211*, 108664. [CrossRef]
45. Chen, L.; Xu, Z.; Wang, F.; Duan, G.; Xu, W.; Zhang, G.; Yang, H.; Liu, J.; Jiang, S. A Flame-Retardant and Transparent Wood/Polyimide Composite with Excellent Mechanical Strength. *Compos. Commun.* **2020**, *20*, 100355. [CrossRef]
46. He, H.; Liu, Q.; Zhang, S.-D.; Chen, H.-B. Fabrication and Properties of Polyimide/Carbon Fiber Aerogel and the Derivative Carbon Aerogel. *Ind. Eng. Chem. Res.* **2022**, *61*, 3952–3961. [CrossRef]
47. Bürger, A.; Fitzer, E.; Heym, M.; Terwiesch, B. Polyimides as Precursors for Artificial Carbon. *Carbon* **1975**, *13*, 149–157. [CrossRef]
48. Chen, W.; Chen, W.; Zhang, B.; Yang, S.; Liu, C.Y. Thermal Imidization Process of Polyimide Film: Interplay between Solvent Evaporation and Imidization. *Polymer* **2017**, *109*, 205–215. [CrossRef]
49. Genovese, A.; Shanks, R.A. Fire Performance of Poly(Dimethyl Siloxane) Composites Evaluated by Cone Calorimetry. *Compos. Part A Appl. Sci. Manuf.* **2008**, *39*, 398–405. [CrossRef]
50. Zhong, H.; Wu, D.; Wei, P.; Jiang, P.; Li, Q.; Hao, J. Synthesis, Characteristic of a Novel Additive-Type Flame Retardant Containing Silicon and Its Application in PC/ABS Alloy. *J. Mater. Sci.* **2007**, *42*, 10106–10112. [CrossRef]
51. Zielecka, M.; Rabajczyk, A.; Pastuszka, Ł.; Jurecki, L. Flame Resistant Silicone-Containing Coating Materials. *Coatings* **2020**, *10*, 479. [CrossRef]

52. Nodera, A.; Kanai, T. Flame Retardancy of Polycarbonate-Polydimethylsiloxane Block Copolymer/Silica Nanocomposites. *J. Appl. Polym. Sci.* **2006**, *101*, 3862–3868. [CrossRef]
53. McGrath, J.E.; Dunson, D.L.; Mecham, S.J.; Hedrick, J.L. Synthesis and Characterization of Segmented Polyimide-Polyorganosiloxanecopolymers. *Adv. Polym. Sci.* **1999**, *140*, 61–105. [CrossRef]
54. Unsal, E.; Cakmak, M. Real-Time Characterization of Physical Changes in Polyimide Film Formation: From Casting to Imidization. *Macromolecules* **2013**, *46*, 8616–8627. [CrossRef]
55. Furukawa, N.; Yamada, Y.; Kimurak, Y. Preparation and Stress Relaxation Properties of Thermoplastic Polysiloxane-Block-Polyimides. *High Perform. Polym.* **1996**, *8*, 617–630. [CrossRef]
56. Lauver, R.W. Kinetics of Imidization and Crosslinking in PMR Polyimide Resin. *J. Polym. Sci. Polym. Chem. Ed.* **1979**, *17*, 2529–2539. [CrossRef]
57. Xiao, S.; Iroh, J.O. Novel Polyimide-Block-Poly(Dimethyl Siloxane) Copolymers: Effect of Time on the Synthesis and Thermal Properties. *High Perform. Polym.* **2021**, *34*, 095400832110404. [CrossRef]
58. He, W.; Song, P.; Yu, B.; Fang, Z.; Wang, H. Flame Retardant Polymeric Nanocomposites through the Combination of Nanomaterials and Conventional Flame Retardants. *Prog. Mater. Sci.* **2020**, *114*, 100687. [CrossRef]
59. Han, Y.; Wu, Y.; Shen, M.; Huang, X.; Zhu, J.; Zhang, X. Preparation and Properties of Polystyrene Nanocomposites with Graphite Oxide and Graphene as Flame Retardants. *J. Mater. Sci.* **2013**, *48*, 4214–4222. [CrossRef]
60. Beyer, G. Short Communication: Carbon Nanotubes as Flame Retardants for Polymers. *Fire Mater.* **2002**, *26*, 291–293. [CrossRef]
61. Beyer, G. Nanocomposites: A New Class of Flame Retardants for Polymers. *Plast. Addit. Compd.* **2002**, *4*, 22–28. [CrossRef]
62. Shi, Y.; Li, L.J. Chemically Modified Graphene: Flame Retardant or Fuel for Combustion? *J. Mater. Chem.* **2011**, *21*, 3277–3279. [CrossRef]
63. Bao, C.; Song, L.; Wilkie, C.A.; Yuan, B.; Guo, Y.; Hu, Y.; Gong, X. Graphite Oxide, Graphene, and Metal-Loaded Graphene for Fire Safety Applications of Polystyrene. *J. Mater. Chem.* **2012**, *22*, 16399–16406. [CrossRef]
64. Wang, X.; Song, L.; Yang, H.; Lu, H.; Hu, Y. Synergistic Effect of Graphene on Antidripping and Fire Resistance of Intumescent Flame Retardant Poly(Butylene Succinate) Composites. *Ind. Eng. Chem. Res.* **2011**, *50*, 5376–5383. [CrossRef]
65. Sang, B.; Li, Z.W.; Li, X.H.; Yu, L.G.; Zhang, Z.J. Graphene-Based Flame Retardants: A Review. *J. Mater. Sci.* **2016**, *51*, 8271–8295. [CrossRef]
66. Wu, Q.; Zhu, W.; Zhang, C.; Liang, Z.; Wang, B. Study of Fire Retardant Behavior of Carbon Nanotube Membranes and Carbon Nanofiber Paper in Carbon Fiber Reinforced Epoxy Composites. *Carbon* **2010**, *48*, 1799–1806. [CrossRef]
67. Dittrich, B.; Wartig, K.-A.; Hofmann, D.; Mülhaupt, R.; Schartel, B. Flame Retardancy through Carbon Nanomaterials: Carbon Black, Multiwall Nanotubes, Expanded Graphite, Multi-Layer Graphene and Graphene in Polypropylene. *Polym. Degrad. Stab.* **2013**, *98*, 1495–1505. [CrossRef]
68. Fu, X.; Zhang, C.; Liu, T.; Liang, R.; Wang, B. Carbon Nanotube Buckypaper to Improve Fire Retardancy of High-Temperature/High-Performance Polymer Composites. *Nanotechnology* **2010**, *21*, 235701. [CrossRef]
69. Morgan, A.B.; Putthanarat, S. Use of Inorganic Materials to Enhance Thermal Stability and Flammability Behavior of a Polyimide. *Polym. Degrad. Stab.* **2011**, *96*, 23–32. [CrossRef]
70. Kausar, A.; Rafique, I.; Muhammad, B. Significance of Carbon Nanotube in Flame-Retardant Polymer/CNT Composite: A Review. *Polym.-Plast. Technol. Eng.* **2017**, *56*, 470–487. [CrossRef]
71. Ruoff, R.S.; Lorents, D.C. Mechanical and Thermal Properties of Carbon Nanotubes. *Carbon* **1995**, *33*, 925–930. [CrossRef]
72. Popov, V. Carbon Nanotubes: Properties and Application. *Mater. Sci. Eng. R Rep.* **2004**, *43*, 61–102. [CrossRef]
73. Kausar, A.; Rafique, I.; Muhammad, B. Review of Applications of Polymer/Carbon Nanotubes and Epoxy/CNT Composites. *Polym.-Plast. Technol. Eng.* **2016**, *55*, 1167–1191. [CrossRef]
74. Ma, H.; Tong, L.; Xu, Z.; Fang, Z. Synergistic Effect of Carbon Nanotube and Clay for Improving the Flame Retardancy of ABS Resin. *Nanotechnology* **2007**, *18*, 375602. [CrossRef]
75. Mukhopadhyay, K.; Ram, K.; Rao, K. Carbon Nanotubes and Related Structures. *Def. Sci. J.* **2008**, *58*, 437–450. [CrossRef]
76. Xu, X.; Cao, J.; Zhang, Y.; Yang, F.; Deng, Y. The Synthesis and Properties of Isocyanate-Based Polyimide Foam Composites Containing MWCNTs of Various Contents and Diameters. *RSC Adv.* **2022**, *12*, 5546–5556. [CrossRef]
77. Kashiwagi, T.; Du, F.; Winey, K.I.; Groth, K.M.; Shields, J.R.; Bellayer, S.P.; Kim, H.; Douglas, J.F. Flammability Properties of Polymer Nanocomposites with Single-Walled Carbon Nanotubes: Effects of Nanotube Dispersion and Concentration. *Polymer* **2005**, *46*, 471–481. [CrossRef]
78. Zhang, T.; Li, W.; Huang, K.; Guo, H.; Li, Z.; Fang, Y.; Yadav, R.M.; Shanov, V.; Ajayan, P.M.; Wang, L.; et al. Regulation of Functional Groups on Graphene Quantum Dots Directs Selective CO2 to CH4 Conversion. *Nat. Commun.* **2021**, *12*, 5265. [CrossRef]
79. Yuan, B.; Fan, A.; Yang, M.; Chen, X.; Hu, Y.; Bao, C.; Jiang, S.; Niu, Y.; Zhang, Y.; He, S.; et al. The Effects of Graphene on the Flammability and Fire Behavior of Intumescent Flame Retardant Polypropylene Composites at Different Flame Scenarios. *Polym. Degrad. Stab.* **2017**, *143*, 42–56. [CrossRef]
80. Li, Y.; Pei, X.; Shen, B.; Zhai, W.; Zhang, L.; Zheng, W. Polyimide/Graphene Composite Foam Sheets with Ultrahigh Thermostability for Electromagnetic Interference Shielding. *RSC Adv.* **2015**, *5*, 24342–24351. [CrossRef]
81. Xu, L.; Jiang, S.; Li, B.; Hou, W.; Li, G.; Memon, M.A.; Huang, Y.; Geng, J. Graphene Oxide: A Versatile Agent for Polyimide Foams with Improved Foaming Capability and Enhanced Flexibility. *Chem. Mater.* **2015**, *27*, 4358–4367. [CrossRef]

82. Çakir, M.; Kılıç, V.; Boztoprak, Y.; Özmen, F.K. Graphene oxide-containing Isocyanate-based Polyimide Foams: Enhanced Thermal Stability and Flame Retardancy. *J. Appl. Polym. Sci.* **2021**, *138*, 51012. [CrossRef]
83. Has, M.; Erdem, A.; Savas, L.A.; Tayfun, U.; Dogan, M. The Influence of Expandable Graphite on the Thermal, Flame Retardant and Mechanical Characteristics of Short Carbon Fiber Reinforced Polyamide Composites. *J. Thermoplast. Compos. Mater.* **2022**, 089270572210966. [CrossRef]
84. Guo, Y.; Bao, C.; Song, L.; Yuan, B.; Hu, Y. In Situ Polymerization of Graphene, Graphite Oxide, and Functionalized Graphite Oxide into Epoxy Resin and Comparison Study of on-the-Flame Behavior. *Ind. Eng. Chem. Res.* **2011**, *50*, 7772–7783. [CrossRef]
85. Mei, X.; Ouyang, J. Ultrasonication-Assisted Ultrafast Reduction of Graphene Oxide by Zinc Powder at Room Temperature. *Carbon* **2011**, *49*, 5389–5397. [CrossRef]
86. Bao, C.; Guo, Y.; Yuan, B.; Hu, Y.; Song, L. Functionalized Graphene Oxide for Fire Safety Applications of Polymers: A Combination of Condensed Phase Flame Retardant Strategies. *J. Mater. Chem.* **2012**, *22*, 23057–23063. [CrossRef]
87. Akinyi, C.; Longun, J.; Chen, S.; Iroh, J.O. Decomposition and Flammability of Polyimide Graphene Composites. *Minerals* **2021**, *11*, 168. [CrossRef]
88. Iji, M.; Serizawa, S. Silicone Derivatives as New Flame Retardants for Aromatic Thermoplastics Used in Electronic Devices. *Polym. Adv. Technol.* **1998**, *9*, 593–600. [CrossRef]
89. Okafor, P.A.; Iroh, J.O. Fabrication of Porous Graphene/Polyimide Composites Using Leachable Poly-Acrylic Resin for Enhanced Electrochemical and Energy Storage Capabilities. *J. Mater. Chem. A* **2015**, *3*, 17230–17240. [CrossRef]
90. Okafor, P.A.; Singh-Beemat, J.; Iroh, J.O. Thermomechanical and Corrosion Inhibition Properties of Graphene/Epoxy Ester-Siloxane-Urea Hybrid Polymer Nanocomposites. *Prog. Org. Coat.* **2015**, *88*, 237–244. [CrossRef]
91. Tian, H.; Yao, Y.; Ma, S.; Fu, L.; Xiang, A.; Rajulu, A.V. Improved Mechanical, Thermal and Flame Resistant Properties of Flexible Isocyanate-Based Polyimide Foams by Graphite Incorporation. *High Perform. Polym.* **2018**, *30*, 1130–1138. [CrossRef]
92. Jeon, I.-Y.; Shin, S.-H.; Choi, H.-J.; Yu, S.-Y.; Jung, S.-M.; Baek, J.-B. Heavily Aluminated Graphene Nanoplatelets as an Efficient Flame-Retardant. *Carbon* **2017**, *116*, 77–83. [CrossRef]
93. Huang, J.; Zhao, Z.; Chen, T.; Zhu, Y.; Lv, Z.; Gong, X.; Niu, Y.; Ma, B. Preparation of Highly Dispersed Expandable Graphite/Polystyrene Composite Foam via Suspension Polymerization with Enhanced Fire Retardation. *Carbon* **2019**, *146*, 503–512. [CrossRef]
94. Longun, J.; Walker, G.; Iroh, J.O. Surface and Mechanical Properties of Graphene-Clay/Polyimide Composites and Thin Films. *Carbon* **2013**, *63*, 9–22. [CrossRef]
95. Longun, J.; Iroh, J.O. Nano-Graphene/Polyimide Composites with Extremely High Rubbery Plateau Modulus. *Carbon* **2012**, *50*, 1823–1832. [CrossRef]
96. Longun, J.; Iroh, J.O. Polyimide/Substituted Polyaniline-Copolymer-Nanoclay Composite Thin Films with High Damping Abilities. *J. Appl. Polym. Sci.* **2013**, *128*, 1425–1435. [CrossRef]
97. Iroh, J.O.; Longun, J. Viscoelastic Properties of Montmorillonite Clay/Polyimide Composite Membranes and Thin Films. *J. Inorg. Organomet. Polym. Mater.* **2012**, *22*, 653–661. [CrossRef]
98. Zuo, L.; Fan, W.; Zhang, Y.; Zhang, L.; Gao, W.; Huang, Y.; Liu, T. Graphene/Montmorillonite Hybrid Synergistically Reinforced Polyimide Composite Aerogels with Enhanced Flame-Retardant Performance. *Compos. Sci. Technol.* **2017**, *139*, 57–63. [CrossRef]
99. Akinyi, C.J.; Iroh, J.O. Heat of Decomposition and Fire Retardant Behavior of Polyimide-Graphene Nanocomposites. *Energies* **2021**, *14*, 3948. [CrossRef]
100. Biteau, H.; Steinhaus, T.; Schemel, C.; Simeoni, A.; Marlair, G.; Bal, N.; Torero, J.L. Calculation Methods for the Heat Release Rate of Materials of Unknown Composition. *Fire Saf. Sci.* **2008**, *9*, 1165–1176. [CrossRef]
101. Müller, M.H.B.; Polder, A.; Brynildsrud, O.B.; Lie, E.; Løken, K.B.; Manyilizu, W.B.; Mdegela, R.H.; Mokiti, F.; Murtadha, M.; Nonga, H.E.; et al. Brominated Flame Retardants (BFRs) in Breast Milk and Associated Health Risks to Nursing Infants in Northern Tanzania. *Environ. Int.* **2016**, *89–90*, 38–47. [CrossRef] [PubMed]
102. Ma, Y.; Li, P.; Jin, J.; Wang, Y.; Wang, Q. Current Halogenated Flame Retardant Concentrations in Serum from Residents of Shandong Province, China, and Temporal Changes in the Concentrations. *Environ. Res.* **2017**, *155*, 116–122. [CrossRef] [PubMed]
103. Shaw, S. Halogenated Flame Retardants: Do the Fire Safety Benefits Justify the Risks? *Rev. Environ. Health* **2010**, *25*, 261–306. [CrossRef] [PubMed]
104. Lu, S.-Y.; Hamerton, I. Recent Developments in the Chemistry of Halogen-Free Flame Retardant Polymers. *Prog. Polym. Sci.* **2002**, *27*, 1661–1712. [CrossRef]
105. Petrova, S.; Soudek, P.; Vanek, T. Flame Retardants, Their Use and Environmental Impact. *Chem. Listy* **2015**, *109*, 679–686.
106. Babushok, V.; Tsang, W. Inhibitor Rankings for Alkane Combustion. *Combust. Flame* **2000**, *123*, 488–506. [CrossRef]
107. Gaan, S.; Sun, G.; Hutches, K.; Engelhard, M.H. Effect of Nitrogen Additives on Flame Retardant Action of Tributyl Phosphate: Phosphorus–Nitrogen Synergism. *Polym. Degrad. Stab.* **2008**, *93*, 99–108. [CrossRef]
108. Hörold, S. Phosphorus Flame Retardants in Thermoset Resins. *Polym. Degrad. Stab.* **1999**, *64*, 427–431. [CrossRef]
109. Jian, S.; Ding, C.; Yang, T.; Zhang, C.; Hou, H. Effect of Trace Diphenyl Phosphate on Mechanical and Thermal Performance of Polyimide Composite Films. *Compos. Commun.* **2018**, *7*, 42–46. [CrossRef]
110. Alongi, J.; Frache, A. Flame Retardancy Properties of α-Zirconium Phosphate Based Composites. *Polym. Degrad. Stab.* **2010**, *95*, 1928–1933. [CrossRef]

111. Feng, H.; Qiu, Y.; Qian, L.; Chen, Y.; Xu, B.; Xin, F. Flame Inhibition and Charring Effect of Aromatic Polyimide and Aluminum Diethylphosphinate in Polyamide 6. *Polymers* **2019**, *11*, 74. [CrossRef] [PubMed]
112. Hergenrother, P.M.; Thompson, C.M.; Smith, J.G.; Connell, J.W.; Hinkley, J.A.; Lyon, R.E.; Moulton, R. Flame Retardant Aircraft Epoxy Resins Containing Phosphorus. *Polymer* **2005**, *46*, 5012–5024. [CrossRef]
113. Peters, E.N. Flame-Retardant Thermoplastics. I. Polyethylene–Red Phosphorus. *J. Appl. Polym. Sci.* **1979**, *24*, 1457–1464. [CrossRef]
114. Granzow, A.; Cannelongo, J.F. The Effect of Red Phosphorus on the Flammability of Poly(Ethylene Terephthalate). *J. Appl. Polym. Sci.* **1976**, *20*, 689–701. [CrossRef]
115. Liu, H.; Guo, Y.; Tian, H.; Yao, Y.; Liu, Q.; Xiang, A.; Zhou, H. Fabrication of Polyimide Foams with Superior Mechanical and Flame Resistance Properties Utilizing the Graft Copolymerization between Red Phosphorus and Graphene Oxide. *Mater. Sci. Eng. B* **2022**, *275*, 115498. [CrossRef]
116. Levchik, S.V.; Costa, L.; Camino, G. Effect of the Fire-Retardant Ammonium Polyphosphate on the Thermal Decomposition of Aliphatic Polyamides. Part III—Polyamides 6.6 and 6.10. *Polym. Degrad. Stab.* **1994**, *43*, 43–54. [CrossRef]
117. Duquesne, S.; le Bras, M.; Bourbigot, S.; Delobel, R.; Camino, G.; Eling, B.; Lindsay, C.; Roels, T.; Vezin, H. Mechanism of Fire Retardancy of Polyurethanes Using Ammonium Polyphosphate. *J. Appl. Polym. Sci.* **2001**, *82*, 3262–3274. [CrossRef]
118. Shih, Y.-F.; Wang, Y.-T.; Jeng, R.-J.; Wei, K.-M. Expandable Graphite Systems for Phosphorus-Containing Unsaturated Polyesters. I. Enhanced Thermal Properties and Flame Retardancy. *Polym. Degrad. Stab.* **2004**, *86*, 339–348. [CrossRef]
119. El Gouri, M.; El Bachiri, A.; Hegazi, S.E.; Rafik, M.; El Harfi, A. Thermal Degradation of a Reactive Flame Retardant Based on Cyclotriphosphazene and Its Blend with DGEBA Epoxy Resin. *Polym. Degrad. Stab.* **2009**, *94*, 2101–2106. [CrossRef]
120. Ding, J.; Shi, W. Thermal Degradation and Flame Retardancy of Hexaacrylated/Hexaethoxyl Cyclophosphazene and Their Blends with Epoxy Acrylate. *Polym. Degrad. Stab.* **2004**, *84*, 159–165. [CrossRef]
121. Feng, H.; Qian, L.; Lu, L. Synergistic Effect of Polyimide Charring Agent and Hexaphenoxycyclotriphosphazene on Improving Fire Safety of Polycarbonate: High Graphitization to Strengthen the Char Layer. *Polym. Adv. Technol.* **2021**, *32*, 1135–1149. [CrossRef]
122. You, G.; Cai, Z.; Peng, H.; Tan, X.; He, H. A Well-Defined Cyclotriphosphazene-Based Epoxy Monomer and Its Application as a Novel Epoxy Resin: Synthesis, Curing Behaviors, and Flame Retardancy. *Phosphorus Sulfur Silicon Relat. Elem.* **2014**, *189*, 541–550. [CrossRef]
123. Xu, G.R.; Xu, M.J.; Li, B. Synthesis and Characterization of a Novel Epoxy Resin Based on Cyclotriphosphazene and Its Thermal Degradation and Flammability Performance. *Polym. Degrad. Stab.* **2014**, *109*, 240–248. [CrossRef]
124. Chen, Y.; Wang, W.; Qiu, Y.; Li, L.; Qian, L.; Xin, F. Terminal Group Effects of Phosphazene-Triazine Bi-Group Flame Retardant Additives in Flame Retardant Polylactic Acid Composites. *Polym. Degrad. Stab.* **2017**, *140*, 166–175. [CrossRef]
125. Zhang, K.; Wu, H.; Wang, T.; Yao, M.; Xie, J.; Jiao, Y. Flame-retardant Effect of Cross-linked Phosphazene Derivatives and Pentaerythritol Derivatives on Polypropylene. *J. Therm. Anal. Calorim.* **2021**, *145*, 3067–3075. [CrossRef]
126. Wang, X.; Li, Q.; Di, Y.; XIng, G. Preparation and Properties of Flame-Retardant Viscose Fiber Containing Phosphazene Derivative. *Fibers Polym.* **2012**, *13*, 718–823. [CrossRef]
127. Devaraju, S.; Selvi, M.; Alagar, M. Synthesis and Characterization of Thermally Stable and Flame Retardant Hexakis(4-Aminophenoxy)Cyclotriphosphazene-Based Polyimide Matrices. *Int. J. Polym. Anal. Charact.* **2018**, *23*, 29–37. [CrossRef]
128. Wu, X.; Jiang, G.; Zhang, Y.; Wu, L.; Jia, Y.; Tan, Y.; Liu, J.; Zhang, X. Enhancement of Flame Retardancy of Colorless and Transparent Semi-Alicyclic Polyimide Film from Hydrogenated-BPDA and 4,4′-Oxydianiline via the Incorporation of Phosphazene Oligomer. *Polymers* **2020**, *12*, 90. [CrossRef]
129. Wu, X.; Wu, L.; Qi, L.; Yin, L.M.; Yang, Y.; Jiang, G.L.; Zhi, X.X.; Zhang, Y.; Liu, J.G.; Wu, J.T. Preparation, Characterization, and Continuous Manufacturing of Nonflammable Colorless and Transparent Semi-Alicyclic Polyimide Film Modified with Phenoxy-Phosphazene Oligomer Flame Retardant. *Express Polym. Lett.* **2021**, *15*, 329–342. [CrossRef]
130. Tao, W.; Hu, X.; Sun, J.; Qian, L.; Li, J. Effects of P–N Flame Retardants Based on Cytosine on Flame Retardancy and Mechanical Properties of Polyamide 6. *Polym. Degrad. Stab.* **2020**, *174*, 109092. [CrossRef]
131. Yuan, C.Y.; Chen, S.Y.; Tsai, C.H.; Chiu, Y.S.; Chen-Yang, Y.W. Thermally Stable and Flame-Retardant Aromatic Phosphate and Cyclotriphosphazene-Containing Polyurethanes: Synthesis and Properties. *Polym. Adv. Technol.* **2005**, *16*, 393–399. [CrossRef]
132. Zhang, X.; Eichen, Y.; Miao, Z.; Zhang, S.; Cai, Q.; Liu, W.; Zhao, J.; Wu, Z. Novel Phosphazene-Based Flame Retardant Polyimine Vitrimers with Monomer-Recovery and High Performances. *Chem. Eng. J.* **2022**, *440*, 135806. [CrossRef]
133. Wang, L.; Yang, B.; Guo, Y.; Zhang, Y.; Wang, N.; Li, F.; Yu, H.; Cui, J.; Guo, J.; Mu, B.; et al. Synthesis of Multielement Phosphazene Derivative and the Study on Flame-Retardant Properties of Epoxy Resin. *High Perform. Polym.* **2020**, *32*, 1169–1180. [CrossRef]
134. Rangaraj, V.M.; Singh, S.; Devaraju, S.; Wadi, V.S.; Alhassan, S.; Anjum, D.H.; Mittal, V. Polypropylene/Phosphazene Nanotube Nanocomposites: Thermal, Mechanical, and Flame Retardation Studies. *J. Appl. Polym. Sci.* **2020**, *173*, 49525. [CrossRef]
135. van Krevelen, D.W. Some Basic Aspects of Flame Resistance of Polymeric Materials. *Polymer* **1975**, *16*, 615–620. [CrossRef]
136. Kumar, D.; Gupta, A.D. Aromatic Cyclolinear Phosphazene Polyimides Based on a Novel Bis-Spiro-Substituted Cyclotriphosphazene Diamine. *Macromolecules* **1995**, *28*, 6323–6329. [CrossRef]
137. Shin, Y.J.; Ham, Y.R.; Kim, S.H.; Lee, D.H.; Kim, S.B.; Park, C.S.; Yoo, Y.M.; Kim, J.G.; Kwon, S.H.; Shin, J.S. Application of Cyclophosphazene Derivatives as Flame Retardants for ABS. *J. Ind. Eng. Chem.* **2010**, *16*, 364–367. [CrossRef]
138. Di, Y.; Wu, X.; Zhao, Z.; Wang, W. Experimental Investigation of Mechanical, Thermal, and Flame-retardant Property of Polyamide 6/Phenoxyphosphazene Fibers. *J. Appl. Polym. Sci.* **2020**, *137*, 48458. [CrossRef]

139. Kirby, R.; Mosurkal, R.; Li, L.; Kumar, J.; Soares, J.W. Polysiloxane-Based Organoclay Nanocomposites as Flame Retardants. *Polym. Plast. Technol. Eng.* **2013**, *52*, 1527–1534. [CrossRef]
140. Lu, Z.; Feng, W.; Kang, X.; Wang, J.; Xu, H.; Wang, Y.; Liu, B.; Fang, X.; Ding, T. Synthesis of Siloxane-containing Benzoxazine and Its Synergistic Effect on Flame Retardancy of Polyoxymethylene. *Polym. Adv. Technol.* **2019**, *30*, 2686–2694. [CrossRef]
141. Mosurkal, R.; Tucci, V.; Samuelson, L.A.; Smith, K.D.; Westmoreland, P.R.; Parmar, V.S.; Kumar, J.; Watterson, A.C. Novel Organo-Siloxane Copolymers for Flame Retardant Applications. In *Advances in Silicones and Silicone-Modified Materials*; American Chemical Society: Washington, DC, USA, 2010; pp. 157–165.
142. Long, J.; Shi, X.; Liu, B.; Lu, P.; Chen, L.; Wang, Y. Semi-Aromatic Polyamides Containing Siloxane Unit toward High Performance. *Acta Polym. Sin.* **2020**, *51*, 681–686.
143. Song, R.; Chang, L.; Li, B. Flame Retardancy and Thermal Properties of Carboxyl-Containing Polysiloxane Derivatives in Polycarbonate. *J. Appl. Polym. Sci.* **2014**, *131*, 39814. [CrossRef]
144. Tian, J.; Yang, Y.; Xue, T.; Chao, G.; Fan, W.; Liu, T. Highly Flexible and Compressible Polyimide/Silica Aerogels with Integrated Double Network for Thermal Insulation and Fire-Retardancy. *J. Mater. Sci. Technol.* **2022**, *105*, 194–202. [CrossRef]
145. Hamdani, S.; Longuet, C.; Perrin, D.; Lopez-cuesta, J.M.; Ganachaud, F. Flame Retardancy of Silicone-Based Materials. *Polym. Degrad. Stab.* **2009**, *94*, 465–495. [CrossRef]
146. Deshpande, G.; Rezac, M.E.; Irisawa, T. The Effect of Phenyl Content on the Degradation of Poly(Dimethyl Diphenyl) Siloxane Copolymers. *Polym. Degrad. Stab.* **2001**, *74*, 363–370. [CrossRef]
147. Jovanovic, J.D.; Govedarica, M.N.; Dvornic, P.R.; Popovic, I.G. The Thermogravimetric Analysis of Some Polysiloxanes. *Polym. Degrad. Stab.* **1998**, *61*, 87–93. [CrossRef]
148. Mansouri, J.; Burford, R.P.; Cheng, Y.B.; Hanu, L. Formation of Strong Ceramified Ash from Silicone-Based Compositions. *J. Mater. Sci.* **2005**, *40*, 5741–5749. [CrossRef]
149. Grassie, N.; Francey, K.F. The Thermal Degradation of Polysiloxanes-Part 3: Poly(Dimethyl/Methyl Phenyl Siloxane). *Polym. Degrad. Stab.* **1980**, *2*, 53–66. [CrossRef]
150. Connell, J.E.; Metcalfe, E.; Thomas, M.J.K. Silicate-Siloxane Fire Retardant Composites. *Polym. Int.* **2000**, *49*, 1092–1094. [CrossRef]
151. Dong, W.; Zhang, X.; Liu, Y.; Wang, Q.; Gui, H.; Gao, J.; Song, Z.; Lai, J.; Huang, F.; Qiao, J. Flame Retardant Nanocomposites of Polyamide 6/Clay/Silicone Rubber with High Toughness and Good Flowability. *Polymer* **2006**, *47*, 6874–6879. [CrossRef]
152. Zhang, X.; Ni, X.; Li, C.; You, B.; Sun, G. Co-Gel Strategy for Preparing Hierarchically Porous Silica/Polyimide Nanocomposite Aerogel with Thermal Insulation and Flame Retardancy. *J. Mater. Chem. A* **2020**, *8*, 9701–9712. [CrossRef]
153. Yang, W.-J.; Wei, C.-X.; Yuen, A.C.Y.; Lin, B.; Yeoh, G.H.; Lu, H.-D.; Yang, W. Fire-Retarded Nanocomposite Aerogels for Multifunctional Applications: A Review. *Compos. Part B Eng.* **2022**, *237*, 109866. [CrossRef]
154. Huang, J.; He, C.; Xiao, Y.; Mya, K.Y.; Dai, J.; Siow, Y.P. Polyimide/POSS Nanocomposites: Interfacial Interaction, Thermal Properties and Mechanical Properties. *Polymer* **2003**, *44*, 4491–4499. [CrossRef]
155. Yan, L.; Fu, L.; Chen, Y.; Tian, H.; Xiang, A.; Rajulu, A.V. Improved Thermal Stability and Flame Resistance of Flexible Polyimide Foams by Vermiculite Reinforcement. *J. Appl. Polym. Sci.* **2017**, *134*, 44828. [CrossRef]
156. Faghihi, K.; Hajibeygi, M.; Shabanian, M. Polyimide–Silver Nanocomposite Containing Phosphine Oxide Moieties in the Main Chain: Synthesis and Properties. *Chin. Chem. Lett.* **2010**, *21*, 1387–1390. [CrossRef]
157. Seckin, T.; Köytepe, S. Synthesis and Characterization of Borax-Polyimide for Flame Retardant Applications. *Macromol. Symp.* **2010**, *296*, 575–582. [CrossRef]
158. Fina, A.; Abbenhuis, H.C.L.; Tabuani, D.; Camino, G. Metal Functionalized POSS as Fire Retardants in Polypropylene. *Polym. Degrad. Stab.* **2006**, *91*, 2275–2281. [CrossRef]
159. Scott, D.W.; Scott, B.D.W. Thermal Rearrangement of Branched-Chain Methylpolysiloxanes1 Branched-Chain Methylpolysiloxanes. *J. Am. Chem. Soc.* **1946**, *68*, 356–358. [CrossRef]
160. Mohamed, M.G.; Kuo, S.W. Functional Polyimide/Polyhedral Oligomeric Silsesquioxane Nanocomposites. *Polymers* **2019**, *11*, 26. [CrossRef]
161. Turgut, G.; Dogan, M.; Tayfun, U.; Ozkoc, G. The Effects of POSS Particles on the Flame Retardancy of Intumescent Polypropylene Composites and the Structure-Property Relationship. *Polym. Degrad. Stab.* **2018**, *149*, 96–111. [CrossRef]
162. Devaraju, S.; Vengatesan, M.R.; Selvi, M.; Kumar, A.A.; Alagar, M. Synthesis and Characterization of Bisphenol-A Ether Diamine-Based Polyimide POSS Nanocomposites for Low K Dielectric and Flame-Retardant Applications. *High Perform. Polym.* **2012**, *24*, 85–96. [CrossRef]
163. Jothibasu, S.; Premkumar, S.; Alagar, M.; Hamerton, I. Synthesis and Characterization of a POSS-Maleimide Precursor for Hybrid Nanocomposites. *High Perform. Polym.* **2008**, *20*, 67–85. [CrossRef]
164. Leu, C.M.; Chang, Y.T.; Wei, K.H. Synthesis and Dielectric Properties of Polyimide-Tethered Polyhedral Oligomeric Silsesquioxane (POSS) Nanocomposites via Poss-Diamine. *Macromolecules* **2003**, *36*, 9122–9127. [CrossRef]
165. Kuo, S.W.; Chang, F.C. POSS Related Polymer Nanocomposites. *Prog. Polym. Sci.* **2011**, *36*, 1649–1696. [CrossRef]
166. Wu, H.; Zeng, B.; Chen, J.; Wu, T.; Li, Y.; Liu, Y.; Dai, L. An Intramolecular Hybrid of Metal Polyhedral Oligomeric Silsesquioxanes with Special Titanium-Embedded Cage Structure and Flame Retardant Functionality. *Chem. Eng. J.* **2019**, *374*, 1304–1316. [CrossRef]
167. Zhai, C.; Xin, F.; Cai, L.; Chen, Y.; Qian, L. Flame Retardancy and Pyrolysis Behavior of an Epoxy Resin Composite Flame-retarded by Diphenylphosphinyl-POSS. *Polym. Eng. Sci.* **2020**, *60*, 3024–3035. [CrossRef]

168. Safarikova, B.; Kalendova, A.; Habrova, V.; Zatloukalova, S.; Machovsky, M. Synergistic Effect between Polyhedral Oligomeric Silsesquioxane and Flame Retardants. In *AIP Conference Proceedings*; American Institute of Physics: College Park, MD, USA, 2014; pp. 106–109.
169. Bourbigot, S.; Duquesne, S.; Fontaine, G.; Bellayer, S.; Turf, T.; Samyn, F. Characterization and Reaction to Fire of Polymer Nanocomposites with and without Conventional Flame Retardants. *Mol. Cryst. Liq. Cryst.* **2008**, *486*, 325–1367. [CrossRef]
170. Xue, M.; Zhang, X.; Wu, Z.; Wang, H.; Ding, X.; Tian, X. Preparation and Flame Retardancy of Polyurethane/POSS Nanocomposites. *Chin. J. Chem. Phys.* **2013**, *26*, 445–450. [CrossRef]
171. Muhammad, S.; Niazi, J.H.; Shawuti, S.; Qureshi, A. Functional POSS Based Polyimide Nanocomposite for Enhanced Structural, Thermal, Antifouling and Antibacterial Properties. *Mater. Today Commun.* **2022**, *31*, 103287. [CrossRef]
172. Handke, M.; Handke, B.; Kowalewska, A.; Jastrzebski, W. New Polysilsesquioxane Materials of Ladder-like Structure. *J. Mol. Struct.* **2009**, *924–926*, 254–263. [CrossRef]
173. Wen-Chang Liaw, K.-P.C. Preparation and Properties of Poly(Imide Siloxane) Segmented Copolymer/Silica Hybrid Nanocomposites. *J. Appl. Polym. Sci.* **2007**, *105*, 809–820. [CrossRef]
174. Feng, Y.; Qi, S.; Wu, Z.; Wang, X.; Yang, X.; Wu, D. Preparation and Characterization of Polyimide/Ladder like Polysiloxane Hybrid Films. *Mater. Lett.* **2010**, *64*, 2710–2713. [CrossRef]
175. Fan, H.; Yang, R. Thermal Decomposition of Polyhedral Oligomeric Octaphenyl, Octa(Nitrophenyl), and Octa(Aminophenyl) Silsesquioxanes. *J. Therm. Anal. Calorim.* **2014**, *116*, 349–357. [CrossRef]
176. Fan, H.; Yang, R. Flame-Retardant Polyimide Cross-Linked with Polyhedral Oligomeric Octa(Aminophenyl)Silsesquioxane. *Ind. Eng. Chem. Res.* **2013**, *52*, 2493–2500. [CrossRef]
177. Pielichowski, K.; Njuguna, J.; Janowski, B.; Pielichowski, J. Polyhedral Oligomeric Silsesquioxanes (POSS)-Containing Nanohybrid Polymers. In *Supramolecular Polymers Polymeric Betains Oligomers*; Springer: Berlin/Heidelberg, Germany, 2006; pp. 225–296.
178. Zhang, M.; Zhang, W.; Chen, Y.; Yang, B. Preparation of Efficiently Intumescent-Flame-Retarded Polypropylene Composite: Synergistic Effect of Novel Phosphorus-Containing Polyhedral Oligomeric Silsesquioxane. *Plast. Rubber Compos.* **2021**, *50*, 464–476. [CrossRef]
179. Strąkowska, A.; Członka, S.; Miedzińska, K.; Strzelec, K. Chlorine-Functional Silsesquioxanes (POSS-Cl) as Effective Flame Retardants and Reinforcing Additives for Rigid Polyurethane Foams. *Molecules* **2021**, *26*, 3979. [CrossRef]
180. Li, S.; Yan, H.; Tang, C.; Niu, S.; Jia, Y. Novel Phosphorus-Containing Polyhedral Oligomeric Silsesquioxane Designed for High-Performance Flame-Retardant Bismaleimide Resins. *J. Polym. Res.* **2016**, *23*, 238. [CrossRef]
181. Song, T.; Li, Z.S.; Liu, J.G.; Yang, S.Y. Novel Phosphorus–Silicon Synergistic Flame Retardants: Synthesis and Characterization. *Chin. Chem. Lett.* **2012**, *23*, 793–796. [CrossRef]
182. Liu, C.; Chen, T.; Yuan, C.; Chang, Y.; Chen, G.; Zeng, B.; Xu, Y.; Luo, W.; Dai, L. Highly Transparent and Flame-Retardant Epoxy Composites Based on a Hybrid Multi-Element Containing POSS Derivative. *RSC Adv.* **2017**, *7*, 46139–46147. [CrossRef]
183. Karlsson, L.; Lundgren, A.; Jungqvist, J.; Hjertberg, T. Effect of Nanofillers on the Flame Retardant Properties of a Polyethylene-Calcium Carbonate-Silicone Elastomer System. *Fire Mater.* **2011**, *35*, 443–452. [CrossRef]
184. Zhang, W.; Li, X.; Guo, X.; Yang, R. Mechanical and Thermal Properties and Flame Retardancy of Phosphorus-Containing Polyhedral Oligomeric Silsesquioxane (DOPO-POSS)/Polycarbonate Composites. *Polym. Degrad. Stab.* **2010**, *95*, 2541–2546. [CrossRef]
185. Jiang, J.; Wang, Y.; Luo, Z.; Qi, T.; Qiao, Y.; Zou, M.; Wang, B. Design and Application of Highly Efficient Flame Retardants for Polycarbonate Combining the Advantages of Cyclotriphosphazene and Silicone Oil. *Polymers* **2019**, *11*, 1155. [CrossRef] [PubMed]
186. Yang, J.; Ma, W.; Hu, D.; Zhang, D.; Wu, L.; Yang, B.; Zhang, S. Facile Preparation and Flame Retardancy Mechanism of Cyclophosphazene Derivatives for Highly flame-retardant Silicone Rubber Composites. *J. Appl. Polym. Sci.* **2021**, *138*, 50297. [CrossRef]
187. Liu, J.; Kong, D.; Dong, C.; Zhang, Z.; Wang, S.; Sun, H.; Lu, Z. Preparation of a Novel P/Si Polymer and Its Synergistic Flame Retardant Application on Cotton Fabric. *Cellulose* **2021**, *28*, 8735–8749. [CrossRef]
188. Hu, Z.; Chen, L.; Zhao, B.; Luo, Y.; Wang, D.-Y.; Wang, Y.-Z. A Novel Efficient Halogen-Free Flame Retardant System for Polycarbonate. *Polym. Degrad. Stab.* **2011**, *96*, 320–327. [CrossRef]
189. Kumar, R.; Tyagi, R.; Parmar, V.S.; Samuelson, L.A.; Kumar, J.; Schoemann, A.; Westmoreland, P.R.; Watterson, A.C. Biocatalytic Synthesis of Highly Flame Retardant Inorganic–Organic Hybrid Polymers. *Adv. Mater.* **2004**, *16*, 1515–1520. [CrossRef]
190. Ni, P.; Fang, Y.; Qian, L.; Qiu, Y. Flame-Retardant Behavior of a Phosphorus/Silicon Compound on Polycarbonate. *J. Appl. Polym. Sci.* **2018**, *135*, 45815. [CrossRef]
191. Hsiue, G.-H.; Liu, Y.-L.; Tsiao, J. Phosphorus-Containing Epoxy Resins for Flame Retardancy V: Synergistic Effect of Phosphorus-Silicon on Flame Retardancy. *J. Appl. Polym. Sci.* **2000**, *78*, 1–7. [CrossRef]
192. Revathi, R.; Prabunathan, P.; Alagar, M. Synthesis and Studies on Phosphazene Core-Based POSS-Reinforced Polyimide Nanocomposites. *Polym. Bull.* **2019**, *76*, 387–407. [CrossRef]
193. Heydari, M.; Rahman, M.; Gupta, R. Kinetic Study and Thermal Decomposition Behavior of Lignite Coal. *Int. J. Chem. Eng.* **2015**, *2015*, 481739. [CrossRef]
194. Serbezeanu, D.; Butnaru, I.; Varganici, C.-D.; Bruma, M.; Fortunato, G.; Gaan, S. Phosphorus-Containing Polyimide Fibers and Their Thermal Properties. *RSC Adv.* **2016**, *6*, 38371–38379. [CrossRef]

195. Othman, M.B.H.; Ahmad, Z.; Osman, H.; Omar, M.F.; Akil, H.M. Thermal Degradation Behavior of a Flame Retardant Melamine Derivative Hyperbranched Polyimide with Different Terminal Groups. *RSC Adv.* **2015**, *5*, 92664–92676. [CrossRef]
196. Buchko, C.J.; Chen, L.C.; Shen, Y.; Martin, D.C. Processing and Microstructural Characterization of Porous Biocompatible Protein Polymer Thin Films. *Polymer* **1999**, *40*, 7397–7407. [CrossRef]
197. Budrugeac, P. Some Methodological Problems Concerning the Kinetic Analysis of Non-Isothermal Data for Thermal and Thermo-Oxidative Degradation of Polymers and Polymeric Materials. *Polym. Degrad. Stab.* **2005**, *89*, 265–273. [CrossRef]
198. Camino, G.; Costa, L.; Casorati, E.; Bertelli, G.; Locatelli, R. The Oxygen Index Method in Fire Retardance Studies of Polymeric Materials. *J. Appl. Polym. Sci.* **1988**, *35*, 1863–1876. [CrossRef]
199. Fenimore, C.P.; Martin, F.J. Flammability of Polymers. *Combust. Flame* **1966**, *10*, 135–139. [CrossRef]
200. Redfern, J.P. Rate of Heat Release Measurement Using the Cone Calorimeter. *J. Therm. Anal.* **1989**, *35*, 1861–1877. [CrossRef]
201. Weil, E.D.; Patel, N.G.; Said, M.M.; Hirschler, M.M.; Shakir, S. Oxygen Index: Correlations to Other Fire Tests. *Fire Mater.* **1992**, *16*, 159–167. [CrossRef]
202. Wang, Y.; Zhang, J.; Jow, J.; Su, K. Analysis and Modeling of Ignitability of Polymers in the UL-94 Vertical Burning Test Condition. *J. Fire Sci.* **2009**, *27*, 561–581. [CrossRef]
203. Wang, Y.; Jow, J.; Su, K.; Zhang, J. Dripping Behavior of Burning Polymers under UL94 Vertical Test Conditions. *J. Fire Sci.* **2012**, *30*, 477–501. [CrossRef]
204. Wang, Y.; Zhang, J. Thermal Stabilities of Drops of Burning Thermoplastics under the UL 94 Vertical Test Conditions. *J. Hazard. Mater.* **2013**, *246–247*, 103–109. [CrossRef] [PubMed]
205. Morgan, A.B.; Bundy, M. Cone Calorimeter Analysis of UL-94 V-Rated Plastics. *Fire Mater.* **2007**, *31*, 257–283. [CrossRef]
206. Dupretz, R.; Fontaine, G.; Duquesne, S.; Bourbigot, S. Instrumentation of UL-94 Test: Understanding of Mechanisms Involved in Fire Retardancy of Polymers. *Polym. Adv. Technol.* **2015**, *26*, 865–873. [CrossRef]
207. Piechota, H. Some Correlations Between Raw Materials, Formalation, and Flame-Retardant Properties of Rigid Urethane Foams. *J. Cell. Plast.* **1965**, *1*, 186–199. [CrossRef]
208. Babrauskas, V. Development of the Cone Calorimeter?A Bench-Scale Heat Release Rate Apparatus Based on Oxygen Consumption. *Fire Mater.* **1984**, *8*, 81–95. [CrossRef]
209. Babrauskas, V.; Parker, W.J. Ignitability Measurements with the Cone Calorimeter. *Fire Mater.* **1987**, *11*, 31–43. [CrossRef]
210. Morgan, A.B.; Benin, V.; Klosterman, D.A.; Sulayman, A.B.; Mukhtar, M.; Galaska, M.L. Organophosphorus-Hydrazides as Potential Reactive Flame Retardants for Epoxy. *J. Fire Sci.* **2020**, *38*, 28–52. [CrossRef]
211. Galaska, M.L.; Horrocks, A.R.; Morgan, A.B. Flammability of Natural Plant and Animal Fibers: A Heat Release Survey. *Fire Mater.* **2017**, *41*, 275–288. [CrossRef]
212. Wang, K.; Morgan, A.B.; Benin, V. Preparation and Studies of New Phosphorus-Containing Diols as Potential Flame Retardants. *Fire Mater.* **2017**, *41*, 973–982. [CrossRef]
213. Zhang, R.; Steiner, M.A.; Agnew, S.R.; Kairy, S.K.; Davies, C.H.J.; Birbilis, N. Experiment-Based Modelling of Grain Boundary β-Phase (Mg2Al3) Evolution during Sensitisation of Aluminium Alloy AA5083. *Sci. Rep.* **2017**, *7*, 2961. [CrossRef]
214. Lyon, R.E.; Walters, R.N.; Stoliarov, S.I.; Safronava, N. *Principles and Practice of Microscale Combustion Calorimetry*; Federal Aviation Administration, Atlantic City Airport: Atlantic City, NJ, USA, 2013; pp. 1–80.
215. Xu, Q.; Mensah, R.A.; Jin, C.; Jiang, L. A Critical Review of the Methods and Applications of Microscale Combustion Calorimetry for Material Flammability Assessment. *J. Therm. Anal. Calorim.* **2021**, *147*, 6001–6013. [CrossRef]